PNAS
www.pnas.org

Supplementary Information for

HOPS-dependent endosomal fusion is required for efficient cytosolic delivery of therapeutic peptides and small proteins

Angela Steinauer,[1] Jonathan R. LaRochelle,[2] Susan L. Knox,[1] Rebecca Wissner,[1] Samuel Berry,[3] and Alanna Schepartz[1,2,*]

[1]Department of Chemistry, Yale University, 225 Prospect Street, New Haven, CT 06520-8107, USA
[2]Department of Molecular, Cellular and Developmental Biology, Yale University, New Haven, CT 06520-8103, USA
[3]Department of Molecular Biophysics and Biochemistry, Yale University, New Haven, CT 06520-8114, USA

*Corresponding author: Alanna Schepartz
Email: alanna.schepartz@yale.edu

This PDF file includes:

Other supplementary materials for this manuscript include the following:

www.pnas.org/cgi/doi/10.1073/pnas.1812044116

Reagents, Chemicals, & Experimental Model Systems

Cell culture. Opti-MEM I reduced serum medium (Gibco, #31985). McCoy's 5A medium with phenol red, without L-glutamine (Sigma, #M8403). McCoy's 5A medium without phenol red (HyClone, #SH30270). Dulbecco's modified eagle medium (DMEM), high glucose (Gibco, #11965). DMEM without phenol red, high glucose, with HEPES (Gibco, #21063). Dulbecco's phosphate buffered saline (DPBS) (Gibco, #14190). Fetal bovine serum (FBS), heat inactivated (Sigma, #F4135). Penicillin streptomycin (pen strep) (Gibco, #15140). GlutaMAX supplement (100X) (Gibco, #35050). Sodium pyruvate (100 mM, 100X) (Gibco, #11360). TrypLE Express (without phenol red) (Gibco, #12604). Fibronectin from bovine plasma (Sigma, #F1141). Lipofectamine 3000 transfection kit (Invitrogen, #L3000). Lipofectamine RNAiMAX reagent (Invitrogen, #13778).

Chemicals. Sucrose, BioUltra, for molecular biology (Sigma, #84097). Dextran, Alexa Fluor 488, 10,000 MW, anionic, fixable (Invitrogen, #D22910). Lissamine rhodamine B ethylenediamine (Thermo Fisher Scientific, #L2424). Lissamine rhodamine B sulfonyl chloride (Acros Organics, #413230010). Alexa Fluor 594 hydrazide (Life Technologies, #A10438). Hoechst 33342, trihydrochloride, trihydrate (Molecular Probes, #H3580). (*R*)-*N*-Fmoc-2-(7'-octenyl)alanine (Fmoc-R8-OH, #OK-UA-09222) and (*S*)-*N*-Fmoc-2-(4'-pentenyl)alanine (Fmoc-S5-OH, #OK-UA-09216) (Okeanos Tech Jiangsu Co.). Silicon rhodamine (SiR)-carboxyl was prepared as described previously (1).

Oligonucleotides. siRNAs and RT-qPCR primers. See Table S3.

Expression Plasmids. The DNA sequences for human galectins (hGal) 3 and 8 were cloned into the 3rd generation lentiviral eGFP expression vector pLenti CMV GFP Puro. The sequence for hGal3 was excised from plasmid pEGFP-hGal3 using restriction enzymes BsrGI-HF (New England Biolabs, #R3575S) and SalI (New England Biolabs, #R0138S) and ligated into the pLenti vector backbone digested with the same restriction enzymes using T4 DNA ligase (New England Biolabs, #B0202S) resulting in the plasmid pLenti CMV eGFP-hGal3 (this paper). The sequence of hGal8 (isoform A, 359 amino acids) was ordered as a codon-optimized gBlock gene fragment from Integrated DNA Technologies (IDT) with overhangs containing restriction enzyme sites for BsrgI-HF and SalI. After double digest and PCR cleanup, this fragment was ligated into the linearized pLenti CMV GFP puro vector using T4 ligase resulting in the plasmid pLenti CMV eGFP-hGal8 (this paper). For lentiviral particles, VSV-G envelope expressing plasmid pMD2.G and 2nd generation lentiviral packaging plasmid psPAX2 were used. pLenti CMV GFP Puro was a gift from Eric Campeau and Paul Kaufman (Addgene plasmid #17448) (2). pEGFP-hGal3 was a gift from Tamotsu Yoshimori (Addgene plasmid #73080) (3). pMD2.G and psPAX2 plasmids were a gift from Didier Trono (Addgene plasmids #12259 and #12260).

Bacterial Strains. For DNA plasmid amplification *Escherichia coli* strain XL10-Gold (Agilent Technologies, #200315) was used and cultured in LB medium.

Cell Lines. All mammalian cell lines were purchased from the American Type Culture Collection. Human osteosarcoma (Saos-2) (ATCC, HTB-85) cells were cultured in McCoy's 5A without L-glutamine supplemented with 15% fetal bovine serum (FBS), 1x GlutaMAX, sodium pyruvate (1 mM), penicillin (100 units/mL), and streptomycin (100 µg/mL). Human embryonic kidney (HEK) 293T cells were cultured in DMEM supplemented with 10% FBS, L-glutamine (2 mM), penicillin (100 units/mL), and streptomycin (100 µg/mL). Cultures were maintained at 37 °C in a humidified atmosphere at 5%, CO_2.

Supplementary Methods

M1. Synthesis of Peptides and Miniature Proteins

Automated Peptide Synthesis. All peptides and miniature proteins were synthesized on H-PAL ChemMatrix or H-Rink ChemMatrix resin on a 50 µmol scale to generate products carrying C-terminal amides. All peptides and miniature proteins were synthesized on an Initiator+ Alstra synthesizer (Biotage) using microwave acceleration. Prior to the first amino acid coupling, the resin was swelled in *N*,*N*-dimethylformamide (DMF) (4.5 mL) at 70 °C for 20 minutes (min). For standard amino acid couplings, DMF (4.5 mL), *N*,*N*,*N*′,*N*′-tetramethyl-*O*-(1*H*-benzotriazol-1-yl)uronium hexafluorophosphate (HBTU) (5.0 equiv.), 1-hydroxybenzotriazole hydrate (HOBt) (5.0 equiv.), *N*,*N*-diisopropylethylamine (DIEA) (10.0 equiv.), and Fmoc-protected amino acid (5.0 equiv.) were subjected to microwave-assisted standard amino acid couplings (75 °C for 5 min). All arginine, cysteine, and histidine residues were coupled at 50 °C. All arginine residues were coupled twice. To couple olefinic residues, DMF (4.5 mL), PyClocK (3.75 equiv.), Fmoc-protected olefinic amino acids (Fmoc-S_5-OH or Fmoc-R_8-OH, 3.75 equiv.) were combined and allowed to stir at room temperature (RT) for 2 hours (h). Residues following olefinic amino acids were coupled twice. Fmoc deprotections were performed using 20% piperidine in DMF (4.5 mL) with microwave assistance (70 °C for 3 min, twice). For peptides containing aspartate or glutamate, 0.1 M HOBt was added to the deprotection solution to minimize aspartimide formation. The resin was washed thoroughly with DMF (four times, 4.5 mL/wash) between each coupling and deprotection step. Following synthesis, the resin was transferred to a custom glass reaction vessel containing a stir bar. To prevent sticking of the resin to glass, both the reaction vessel and stir bar were coated with SigmaCote before the resin was added.

Peptide Modifications: N-terminally SDex-Labeled Peptides. $\mathbf{1}^{Dex}$ and **$\mathbf{2}^{Dex}$** CPMPs were synthesized and purified as described before (4). Briefly, Boc-Lys(Fmoc)-OH was coupled onto the N-terminus of a resin-bound peptide in a custom glass vessel using the peptide coupling conditions described above. The Fmoc-protected Lys sidechain was deprotected with 20% piperidine in DMF containing 0.1 M HOBt. Following Fmoc deprotection, dexamethasone-21-thiopropionic acid (SDex) (2.5 equiv.), 1-hydroxy-7-azabenzotriazole (HOAt) (2.5 equiv.), 1-[Bis(dimethylamino)methylene]-1*H*-1,2,3-triazolo[4,5-*b*]pyridinium 3-oxid hexafluorophosphate (HATU) (2.5 equiv.), DIEA (10.0 equiv.) and 2,6-lutidine (7.0 equiv.) in DMF (3.0 mL) were added to the resin. The resin-containing glass vessel was shaken for 18 h at RT on an orbital shaker. The resin was then thoroughly washed with DMF, dichloromethane (DCM), and methanol (MeOH), after which it was dried under a stream of nitrogen overnight.

Peptide Modifications: Hydrocarbon-Stapled Peptides. Hydrocarbon-stapled peptide variants of SAH-p53-8 (**3**) bearing an N-terminal acetyl group or an N-terminal lissamine rhodamine B linked at a Lys side chain were synthesized and purified as described before (5, 6). Briefly, to couple olefinic residues, DMF (4.5 mL), PyClocK (3.75 equiv.), and Fmoc-protected olefinic amino acids (Fmoc-S_5-OH or Fmoc-R_8-OH, 3.75 equiv.) were combined and allowed to stir at RT for 2 h. Residues following olefinic amino acids were coupled twice. Following automated peptide synthesis, resin-bound stapled peptides were washed three times with dichloroethane (DCE) (10 mL) and cyclized on resin in a custom glass vessel, immediately prior to acetylation or rhodamine labeling, using Grubbs Catalyst I (20 equiv.) in DCE (4 mL) for 2 h under a constant stream of nitrogen. This cyclization step was repeated an additional time.

Peptide Modifications: N-Terminal Acetylation. N-terminally acetylated peptides were generated by treating the terminally Fmoc-deprotected resin-bound peptide with a mixture containing acetic anhydride, DIEA, and DMF (2 mL, in a 85:315:1600 volumetric ratio) and stirring at RT for 45 min in a custom glass vessel.

Peptide Modifications: N-Terminal Lissamine Rhodamine B Labeling. To label polypeptides with lissamine rhodamine B, Boc-Lys(Fmoc)-OH or—for stapled peptides—Fmoc-β-Ala-OH was appended to the N-terminus of the respective sequence by combining the N-terminally deprotected resin with 7-azabenzotriazol-1-yloxy)trispyrrolidinophosphonium hexafluorophosphate (PyAOP) (5.0 equiv.), HOAt (5.0 equiv.), and DIEA (10.0 equiv.) in DMF (4 mL) under microwave irradiation in a MARS-5 microwave-accelerated system (CEM Corporation) for 20 min or at RT without microwave irradiation for 45 min. Then, the N-terminal residue was deprotected twice with 25% piperidine in DMF (5 mL) for 10 min each at RT. Following deprotection, the resin was washed thoroughly with alternating DMF (5 mL) and DCM (5 mL), three times, and then with DMF (5 mL), six times. Finally, the peptide synthesis vessel was purged with nitrogen and the resin was washed an additional five times with anhydrous DMF (4 mL) under nitrogen atmosphere. Lissamine rhodamine B sulfonyl chloride (10 equiv.) was solubilized in anhydrous DMF (3 mL) and added directly to the resin after the final anhydrous DMF wash, followed by the addition of anhydrous DIEA (10 equiv.). The reaction vessel was purged with nitrogen, sealed, and covered with aluminum foil to minimize light exposure. The labeling reaction was occur overnight at RT while shaking on an orbital shaker. After labeling, the resin was washed thoroughly with alternating DMF (10 mL) and DCM (10 mL), three times, then extensively with DMF until no excess lissamine rhodamine B was observed in the wash solution. To shrink the resin, it was washed with MeOH (5 mL) twice. Finally, the resin was dried under a stream of nitrogen overnight.

Peptide Modifications: N-to-C Cyclization. N-to-C cyclized peptide CPP12 (5) was synthesized and purified as described before (7). Briefly, the cyclization of the peptide was achieved by incorporating a main chain alloc-protected glutamic acid residue at the C-terminus of the peptide. The allyl group was removed selectively by treatment with $Pd(PPh_3)_4$ (0.1 equiv.), phenylsilane (10 equiv.) in anhydrous DCM (three times, 15 min each) releasing the C-terminal carboxylate. After allyl deprotection, the N-terminal Fmoc group was removed with piperidine (25%) in DMF and the peptide was cyclized by treatment with (benzotriazol-1-yloxy)tripyrrolidinophosphonium

hexafluorophosphate (PyBOP) (5 equiv.), HOBt (5 equiv.) and DIEA (10 equiv.) in DMF overnight (16 h).

Peptide Cleavage from Resin. Once peptide synthesis was complete, the resin was washed thoroughly with alternating DMF (10 mL) and DCM (10 mL), three times, and with MeOH (5 mL), after which it was dried overnight under nitrogen. The peptide was cleaved from the resin using 4 mL (per 50 μmol) of a cocktail containing trifluoroacetic acid (TFA) (88%), phenol (5%), water (5%), and triisopropylsilane (TIPS) (2%) for 3 h at RT. For peptides containing cysteines, the cocktail consisted of TFA (81.5%), thioanisole (5%), phenol (5%), water (5%), ethanedithiol (2.5%), and TIPS (1%). SDex-labeled peptides were cleaved with a cocktail consisting of TFA (92.5%), water (2.5%), TIPS (2.5%), and 3,6-dioxa-1,8-octanedithiol (2.5%). Cleaved peptides were precipitated in diethyl ether (40 mL, chilled to –80 °C), pelleted by centrifugation, redissolved in a mixture of water and acetonitrile (ACN) (max. 20% ACN), frozen, lyophilized to dryness, and reconstituted in 1–2 mL dimethyl sulfoxide (DMSO) prior to purification by high-performance liquid chromatography (HPLC).

Peptide Purification by HPLC. Peptide solutions in DMSO were filtered through nylon syringe filters (0.45 μm, 4 mm from Thermo Fisher Scientific) prior to HPLC purification. All peptides were purified using an Agilent 1260 Infinity HPLC system, a reverse phase Triaryl-C18 (YMC-Triaryl-C18, 150 mm x 10 mm, 5 μm, 12 nm) column (YMC America, Inc.) and eluent gradients of water in ACN containing 0.1% TFA. Peptides were detected at 214 and 280 nm. For lissamine rhodamine B (R)- and silicon rhodamine (SiR)-labeled peptides were also detected at 560 nm and at 645 nm, respectively. Peptide purity was verified using a Shimadzu Analytical ultra-performance liquid chromatography (UPLC) system (ES Industries, Shimadzu Corporation) and a C8 reverse phase (Sonoma C8(2), 3 μm, 100 Å, 2.1 x 100 mm) or a C18 reverse phase (Agilent Poroshell 120, 2.7 μm, 4.5 x 50 mm) analytical column. Analytical samples were eluted using solvent gradients of water in ACN containing 0.1% TFA over 20–25 min and were detected at 214, 280, and, for R- and SiR-labeled peptides, at 560 nm and 645 nm, respectively.

Mass Spectrometry. The molecular mass of each peptide was determined by liquid chromatography-mass spectrometry (LC-MS), using a Waters XEVO Q-TOF mass spectrometer equipped with an Acquity UPLC BEH C18 1.7 μm column (for Chemdraw structures and mass spectrometry data of all peptides see Fig. S1 and Table S1, respectively).

Peptide Reconstitution, Concentration Determination, and Storage. Purified, unlabeled peptides containing tyrosine or tryptophan were dissolved in water and the concentration of the solution was determined using the extinction coefficient of the peptide at 280 nm (ε_{280}), which was estimated using the ProtParam peptide properties calculator on the ExPASy Proteomics Server. For SDex-labeled peptides, concentrations were measured using an SDex extinction coefficient of 12,000 cm^{-1} M^{-1} at 242 nm in water, as described previously (4, 8). For R-labeled peptides, the extinction coefficient for lissamine rhodamine B diethylamine was determined in DPBS (pH 7.4) at 25 °C to be 112,000 ± 2,000 cm^{-1} M^{-1} at λ_{max}(569 nm). This extinction coefficient was used for all rhodamine-labeled peptides. For unlabeled cyclic peptide CPP12, the extinction coefficient of naphthylalanine (3,936 cm^{-1} M^{-1} at λ_{max}(280 nm)) was used (9). For SiR-

labeled peptides, the reported extinction coefficient was used (1). The concentration of unlabeled D-Arg8 (**4**^{UL}) solutions were determined by measuring the mass of the peptide before dissolving it in Milli-Q water. Purified zinc finger CPMPs (**2**^{UL}, **2**^{Dex}, and **2**^{R}) were dissolved in argon-purged 10 mM Tris buffer, pH 7.4. To reduce cysteines, DTT (2 equiv.) was added and the solution was left to react for 15 min. Then, $ZnCl_2$ (2 equiv.) was added to the solution to induce the typical zinc finger fold. Zinc finger peptides were stored in solution at 4 °C. Repeated freeze-thawing cycles of zinc finger and aPP-based miniature proteins were avoided due to peptide aggregation and precipitation. All other peptides (**3**–**5**) were stored as a lyophilized powder or in solution at –20 °C and tolerated repeated freeze-thaw cycles. All peptides were routinely assessed for identity and purity by LC-MS and UPLC analyses.

M2. Fluorescence Correlation Spectroscopy (FCS)

Determination of the Confocal Volume by FCS

FCS measurements were performed on an LSM 880 Airyscan system NLO/FCS confocal microscope (Zeiss) with a C-apochromat 40x N1.2 UV-VIS-IR Korr. water immersion objective (Zeiss), with a gallium arsenide phosphide (GaAsP) detector. The Alexa 594 standard and lissamine rhodamine B-labeled CPMPs and CPPs were excited at 561 nm, and the fluorescence filters were set to 570–660 nm. Measurements were made in 8-well chambered Lab-Tek 8-well coverglass slides (Thermo Fisher Scientific, #155411). Diffusion coefficients of CPMPs and CPPs **1**^{R}–**5**^{R} in buffer were measured at 37 °C in serum-free DMEM without phenol red containing 25 mM HEPES (pH 7.2). Experiments in cultured Saos-2 cells were performed at 37 °C in serum-free DMEM without phenol red containing 25 mM HEPES (pH 7.2). Autocorrelation data were collected over 5-s intervals with 10 repeats. Prior to FCS measurements in cells, the microscope was calibrated using Alexa Fluor 594 hydrazide dye (Life Technologies, #A10438). The coverglass thickness of each 8-well microscopy dish was measured with a digital micrometer (Mitutoyo) to adjust the correction collar of the C-apochromat 40x N1.2 water immersion objective to the correct thickness. The pinhole of the 561 nm laser was aligned in both the x and the y direction. A standard solution of Alexa Fluor 594 hydrazide in Milli-Q water (100 nM) was measured at 37 °C in the same 8-well coverglass slide used for FCS experiments in cultured cells with one well reserved for Alexa Fluor 594 standard (no fibronectin coating). Autocorrelations were fit to diffusion equations described below, using custom MATLAB scripts (Version R2017a, MathWorks), as described before (5, 10, 11).

Autocorrelation curves from measurements in buffer were fit to a 3D diffusion equation (Equation 1):

$$G(\tau) = \frac{1}{N} \cdot \frac{1}{\left(1+\frac{\tau}{\tau_{diff}}\right) \cdot \sqrt{\left(1+\frac{S^2\tau}{\tau_{diff}}\right)}} \qquad \text{(Equation 1)}$$

N is the average number of diffusing molecules in the effective confocal volume (V_{eff}) and τ_{diff} is the diffusion time, the average time a molecule takes to transit the laser focus. The shape factor S of the effective confocal volume V_{eff} was determined from the fit of the autocorrelation function

of Alexa 594 (12.5 nM) in water at 25 °C (S = 0.200 ± 0.007) and was fixed for all subsequent analyses at S = 0.2. V_{eff} was calculated according to Equations 2 and 3:

$$\omega_1 = \sqrt{(4\ D\ \tau_{diff})} \quad \text{(Equation 2)}$$

$$V_{eff} = \pi^{\frac{3}{2}}\ \omega_1^3 \frac{1}{S} \quad \text{(Equation 3)}$$

D is the diffusion coefficient of Alexa 594 at 37 °C (5.20 x 10^{-6} cm^2 s^{-1}) and τ_{diff} is the measured diffusion time. The confocal volume V_{eff} ranged from 0.57–0.75 femtoliters.

The diffusion coefficient D of Alexa 594 at 37 °C was calculated using Equation 4:

$$D(T) = D(25\ °C) \cdot \frac{t+273.15}{\eta(t)} \cdot 2.985 \cdot 10^{-6}\ Pa \cdot s \cdot K^{-1} \quad \text{(Equation 4)}$$

Where t = 37 °C, D of Alexa 594 at is 25 °C (3.88 x 10^{-6} cm^2 s^{-1}) (12), and the viscocity η of water at 37 °C is 0.6913 mPa s.

The final concentration C in the effective confocal volume V_{eff} was calculated as follows (Equation 5):

$$C = \frac{N}{N_A \cdot V_{eff}} \quad \text{(Equation 5)}$$

Where N_A is Avogardro's number (6.0221413 x 10^{23} mol^{-1}).
Autocorrelation curves from *in cellulo* measurements were fit to an anomalous diffusion model:

$$G(\tau) = \frac{1}{N} \cdot \frac{1}{\left(1+\frac{\tau}{\tau_{diff}}\right)^{\alpha} \cdot \sqrt{\left(1+S^2\frac{\tau}{\tau_{diff}}\right)^{\alpha}}} + G(\infty) \quad \text{(Equation 6)}$$

$G(\infty)$ represents the level of background autocorrelation at long time scales and α is the anomalous diffusion coefficient, which represents the degree to which diffusion is hindered over long distances (13).

The fit autocorrelation traces from live-cell measurements were then evaluated and filtered as described before (5). Briefly, for follow-up analysis, we selected traces displaying diffusion times (τ_{diff}) of up to 10-fold of the observed value for the identical CPMP/CPP in buffer. We discarded traces that displayed poor signal with counts per molecule (cpm) below 1 kHz and/or low anomalous diffusion coefficients ($\alpha < 0.3$) (14). With these parameters, we typically retained at least 75% of the collected data points.

Calculation and Measurement of Diffusion Coefficients of CPMPs and CPPs 1^R–5^R
The theoretical diffusion coefficient of a spherical, globular macromolecule can be determined from its respective molecular weight. First, its molecular mass (m) is converted to the

hydrodynamic radius (r) with the following relationship (Equation 7):

$$r = \sqrt[3]{\frac{3m/N_A}{4\pi\rho}} \quad \text{(Equation 7)}$$

Where ρ is mean density, which is 1.2 g/cm^3 for proteins.

Second, the theoretical diffusion coefficient (D) is calculated from r with the Stokes-Einstein equation (Equation 8):

$$D = \frac{kT}{6\pi\eta r} \quad \text{(Equation 8)}$$

k is the Boltzmann constant (1.381 x 10^{-16} erg x K^{-1}), η the viscosity of water at 25 °C (0.891 g m^{-1} s^{-1}), and T is the absolute temperature.

The diffusion coefficients of CPMPs and CPPs $\mathbf{1}^R$–$\mathbf{5}^R$ was measured *in vitro* at 37 °C in serum-free DMEM without phenol red containing 25 mM HEPES (pH 7.2) (Table S2).

M3. Cell-Based Assays

Preparation of eGFP-hGal3 and eGFP-hGal8 Lentiviral Particles for Transduction. HEK 293T cells (ATCC, CRL-3216) were cultured in complete growth medium (DMEM containing 4.5 g/L glucose, phenol red, 10% FBS, 5 mM sodium pyruvate, without antibiotics). Lentiviral particles were prepared in HEK 293T cells using Lipofectamine 3000 (Invitrogen, #L3000) transfection reagent according to the manufacturer's protocol. Briefly, 293T cells were seeded (1.2 Mio/well) into tissue-culture treated 6-well dishes in 2 mL packaging medium (Opti-MEM I containing 5% FBS and 1 mM sodium pyruvate) and left to adhere overnight. For transfection, a 1:1 mixture of solution A containing Lipofectamine 3000 in Opti-MEM I (250 µL) and solution B containing P3000 reagent, psPAX2 (0.24 pmol) and pMD2.G packaging plasmids (0.14 pmol), and either eGFP-hGal3 or eGFP-hGal8 in pLenti CMV GFP puro plasmids (0.12 pmol) in Opti-MEM I (250 µL), was prepared and incubated for 10 min at RT. The 1:1 mixture was added dropwise to the plated HEK 293T cells (total 500 µL/well) in 6-well plates. The medium was replaced with packaging medium 6 h after transfection. Lentiviral particles were harvested 24 h after transfection by carefully collecting the cell supernatant from each well. Wells were replenished with fresh packaging medium, which was collected a second time 52 h post transfection. All lentivirus-containing fractions were stored at 4 °C for two days, combined, filtered through a 0.45 µm pore syringe filter, and concentrated using spin-filter concentrators (Amicon Ultra-15, 100 kD MWCO, EMD Millipore, #UFC910024). The concentrated lentiviral stock solutions were split into aliquots and frozen at –80 °C until used. To determine the viral titer, cells were transduced with increasing amounts of the lentiviral solution and the fluorescence intensity at 509 nm was measured and compared to untreated cells using an Attune NxT flow cytometer (Life Technologies).

Galectin-Based Assay to Measure Endosomal Damage. To begin, 8-well microscopy slides (Thermo Scientific, #155411) were coated with fibronectin from bovine plasma in DPBS (1:100 dilution, 200 µL/well) for 1 h at 37 °C (200 µL/well). The fibronectin solution was removed by aspiration and the dishes were washed three times with DPBS before use. Saos-2 cells were seeded (15,000 cells/well) into the fibronectin-coated dishes in complete McCoy's 5A medium without phenol red (200 µL/well, 15% FBS, 1 mM sodium pyruvate, without P/S) and left to adhere overnight (16 h). Cells were transduced with eGFP-hGal3 or eGFP-hGal8 at a lentiviral particle concentration determined to yield >50% transduced cells as measured by flow cytometry compared to a mock-transduced cell population. After a 16-h transduction period, the medium was removed, cells were washed with DPBS twice, and incubated with pre-warmed clear McCoy's 5A medium without phenol red (without FBS, without sodium pyruvate, without P/S) containing medium only (control), Lipofectamine RNAiMAX (16 µL/mL), LLOMe (1 mM), or CPP/CPMPs **1**–**5** (600 nM) for 1 h at 37 °C, 5% CO_2. Cells were washed three times with pre-warmed DPBS and incubated with HEPES-containing clear DMEM without phenol red (25 mM HEPES, without P/S, without FBS, without sodium pyruvate) for 30 min at 37 °C, 5% CO_2, after which they were imaged by confocal microscopy at 37 °C on a Zeiss laser scanning microscope (LSM 880). For galectin recruitment assays, careful attention was paid not to overexpose cells to allow detection of even small amounts of galectin recruitment to endosomal membranes. To quantify endosomal recruitment, an endosomal recruitment coefficient (ERC) was determined by measuring the area of punctate fluorescence in each cell, dividing it by the overall area of the same cell, and then multiplying it by 10,000 (Fig. S2C) using ImageJ (15). The ERC represents the %-area of punctate fluorescence in each cell multiplied by 100.

CellTiter-Glo Luminescent Cell Viability Assay. Saos-2 cells were seeded into 96-well plates (Corning, #3603; 3000 cells/well, 100 µL/well) in complete McCoy's 5A medium without phenol red (10% FBS, without P/S, 1 mM sodium pyruvate) and left to adhere overnight (16 h). The next day, the medium was replaced with clear McCoy's 5A medium without phenol red (100 µL/well, without FBS, without P/S, without sodium pyruvate) and CPMPs and CPPs $\mathbf{1}^{UL}$–$\mathbf{5}^{UL}$ were added in triplicate to each well at increasing concentrations (0.0, 0.3, 0.6, 1.2, 2.4, 4.8, 9.6, 19.2 µM). Cells were left to incubate at 37 °C, 5% CO_2 for 4 h. CellTiter-Glo (Promega, #G7571) luminescent substrate was added to each well (50 µL/well). The plates were orbitally shaken for 15 min and the resulting luminescence was recorded with a Biotek Synergy 2 plate reader.

FCS-Based Assay to Measure Endosomal Damage Using $\mathbf{Lys9^R}$. One day prior to the experiment, Saos-2 cells were seeded in tissue culture-treated 6-well plates (100,000 cells/well) in complete McCoy's 5A medium without phenol red (2 mL/well, 15% FBS, 1 mM sodium pyruvate, without P/S). The day of the experiment, the medium was removed and cells were washed twice with DPBS. Cells were incubated with $Lys9^R$ (600 nM) in clear McCoy's 5A without phenol red (1 mL/well, without FBS, without sodium pyruvate, without P/S) for 30 min at 37 °C, 5% CO_2. While cells were incubating, an 8-well microscopy slide (Thermo Scientific, #155411) was coated with fibronectin from bovine plasma in DPBS (1:100 dilution, 200 µL/well) for 1 h at 37 °C (200 µL/well). The fibronectin solution was removed by aspiration and the dish was washed three times with DPBS before use. After the 30-min incubation period, cells were washed three times with DBPS and incubated with increasing concentrations of Lipofectamine

RNAiMAX (0, 4, 8, 12, 16 µL/mL), LLOMe (0, 0.125, 0.25, 0.5, 1.0 mM), or unlabeled CPMPs and CPPs **1**^{UL}–**5**^{UL} (300, 600, 1200, 2400 nM) in clear McCoy's 5A without phenol red for 1 h at 37 °C, 5% CO_2 (Fig. S4A). Nuclei were labeled with Hoechst 33342 (300 nM) for 5 min at the end of the 1-h incubation period by adding the nuclear stain directly to the reagent-containing medium. To remove exogenously bound peptide, cells were washed three times with DBPS and treated with TrypLE Express (500 µL/well) for 10 min until all cells were lifted from the culture dish. The cells were transferred to 15-mL Falcon tubes, each well was rinsed twice with complete McCoy's 5A without phenol red (twice, 1 mL each), and the cell suspensions, including media used for rinsing, were pooled and pelleted at 200 *g* for 3 min. The supernatant was removed and cells were resuspended in HEPES-containing clear DMEM without phenol red (1 mL, 25 mM HEPES, without FBS, without sodium pyruvate, without P/S) to wash the pellet. The cells were pelleted again at 200 *g* for 3 min. The supernatant was removed and the cells were resuspended in HEPES-containing clear DMEM without phenol red (600 µL). Of this suspension, one third (200 µL) was plated into the prepared fibronectin-coated microscopy dish. The cells were then left to adhere at 37 °C, 5% CO_2 for 20 min before FCS experiments were performed.

Before beginning experiments at the LSM 880, the live-cell chamber was equilibrated to 37 °C, and the 561-nm (0.5%) laser line warmed up, both for approximately 30 min. After *in vitro* calibration with Alexa 594, confocal images of Saos-2 cells were obtained. FCS measurements were obtained by positioning the 561-nm laser's crosshair in the nucleus or the cytosol of Saos-2 cells. A minimum of 20 cells was measured for each experimental condition. To minimize background fluorescence and artifacts from diffusion, the laser's confocal volume was placed in a cytosolic area devoid of bright endosomes. Measurements in the nucleus were less prone to diffusional artifacts. For each FCS measurement, ten consecutive five-second time intervals were recorded. These ten traces were converted to their corresponding autocorrelation curves using a custom MATLAB script (5). Low quality traces were discarded as described above, the remaining traces were averaged, and the averaged trace was fit to an anomalous diffusion model (Equation 6). From the fit of the averaged autocorrelation curve, we obtained the number of Lys9^R molecules in the focal volume of the laser. This number of Lys9^R molecules was converted to the effective cytosolic or nuclear Lys9^R concentration using the laser's measured focal volume, as described in equations 2–5 above.

FCS-Based Control Experiment With Lys9^{UL}. Except for two modifications, the same experimental protocol was followed as for the experiment with labeled Lys9^R, described above. Instead of Lys9^R, cells were incubated with or without Lys9^{UL} (600 nM), and instead of unlabeled CPMP/CPPs **1**^{UL}–**5**^{UL}, cells were incubated with RhoB-tagged CPMP/CPPs **1**^{R}–**3**^{R} (300, 600, 1200, 2400 nM) (Fig. S4A). We were unable to perform controls that used FCS to evaluate release of RhoB-tagged CPPs **4**^{R} and **5**^{R} in the presence of Lys9^{UL}. Instead, we performed these experiments using a fractionation protocol.

Cytosolic Fractionation to Quantify Cytosolic Access of D-Arg8^R (4^R) and CPP12^R (5^R). When we incubated Saos-2 cells with D-Arg8^R (**4**^{R}) and CPP12^R (**5**^{R}), and performed FCS experiments similar to the ones described for **1**^{R}–**3**^{R} above, we observed *in cellulo* diffusion times that were more than 50 times longer compared to diffusion times commonly observed for aPP5.3^R

(**1**^{R}), ZF5.3^{R} (**2**^{R}), or SAH-p53-8^{R} (**3**^{R}) (Table S2). Such a large increase in diffusion time may be a sign of supramolecular aggregation or binding to intracellular factors, which made it impossible to calculate concentrations from the FCS data. Therefore, we turned to our previously described cytosolic fractionation assay to calculate the cytosolic concentration of **4**^{R} and **5**^{R} relative to **2**^{R}. We performed a nearly identical incubation protocol as described for the FCS-based assays with Lys9 above, however, we started with a larger population of Saos-2 cells. Briefly, one day prior to the experiment, Saos-2 cells were plated in tissue culture-treated 100-mm dishes (1.5 x 10^6 cells/dish) in complete McCoy's 5A without phenol red (5 mL/dish, 15% FBS, 1 mM sodium pyruvate, without P/S). The next day, the medium was removed and cells were washed twice with DPBS. The cells were incubated with or without Lys9^{UL} (600 nM) in clear McCoy's 5A without phenol red (5 mL/well, without FBS, without sodium pyruvate, without P/S) for 30 min at 37 °C, 5% CO_2. After the 30-min incubation, cells were washed three times with DBPS, and incubated with increasing concentrations of RhoB-tagged peptides **2**^{R}, **4**^{R}, or **5**^{R} (300, 600, 1200, 2400 nM) in clear McCoy's 5A medium without phenol red for 1 h at 37 °C, 5% CO_2. To remove exogenously bound peptide, cells were washed three times with DBPS and treated with TrypLE Express (1 mL/dish) for 10 min until all cells were lifted from the culture dish. Cells were transferred to 15-mL Falcon tubes, each well was rinsed twice with complete McCoy's 5A without phenol red (twice, 1 mL each), and the cell suspensions, including the media used for rinsing, were pooled and pelleted at 200 *g* for 3 min. The cells were washed with DPBS (1 mL) twice and pelleted at 200 *g* for 3 min. The cells were resuspended in 1 mL pre-cooled buffered isotonic sucrose buffer (290 mM sucrose, 10 imidazole pH 7.0, added immediately prior to use: 1 mM DTT and 1 cOmplete protease inhibitor cocktail per 10 mL buffer). A 20-uL aliquot was removed for counting, then the suspension was pelleted again at 200 *g* for 3 min. Saos-2 cells were counted using an automated cell counter (Auto T4, Cellometer). The supernatant was removed and cells were suspended in pre-cooled buffered isotonic sucrose to reach a concentration of 10,000 cells/µL. For each experimental condition, 1.5 x 10^6 cells were suspended in 150 µL isotonic sucrose, transferred to a 0.5-mL microtube containing 1.4mm ceramic beads (Omni International, #19-626), and stored on ice for transport. Cells were homogenized using a Bead Ruptor 4 (Omni International) at speed 1 for 10 seconds. The homogenized cells were transferred to Beckman polycarbonate ultracentrifuge tubes (0.2 mL, Beckman Coulter, #343775) and sedimented using a Beckman tabletop ultracentrifuge at 350 K*g* for in an ultracentrifuge (TL-100; Beckman Coulter) for 30 min at 4 °C using a TLA-100 rotor (20 x 0.2 mL). The supernatant (= cytosolic fraction) was analyzed in a 96-well plate (NBS-treated, low-protein binding, Corning, #3651) on a fluorescence plate reader (infinite F500, Tecan) with excitation at 535 ± 25 nm and an emission at 590 ± 20 nm. The concentration of the protein conjugate in the cytosol was calculated using a calibration curve. For the calibration curve, known concentrations of peptides **2**^{R}, **4**^{R}, and **5**^{R} between 1.0 and 1000.0 nM were added to cytosolic extracts of the untreated negative control cells. For background subtraction, several wells containing cytosolic extracts from untreated cells were averaged. The average background fluorescence intensity was subtracted from each well.

Screen Optimization: Seeding Density and Growth Medium. To evaluate the effect of seeding density and the choice of RNAi growth medium on the translocation ratio (TR) of Saos-2(GIGT) cells, Saos-2(GIGT) cells were plated at various seeding densities in either 50 µL of complete

growth medium (McCoy's 5A, with pen/strep, 15% FBS) or transfection medium (complete growth medium/Opti-MEM/RNAi duplex buffer, 3:1:1) in 384-well plates (#1052, Nexus Biosystems). Saos-2(GIGT) cells were allowed to adhere and remain in the respective media for 48 h, after which the cells were serum-starved overnight (16 h), by replacing the media with 40 µL of serum-free DMEM. The following morning, cells were treated with DMEM containing either 1 µM Dex or Dex-peptide conjugate ($\mathbf{1}^{Dex}$ or $\mathbf{2}^{Dex}$) for 30 min, after which cells were fixed with 4% paraformaldehyde for 20 min at RT, stained with the nuclear stain Hoechst 33342 (300 nM) for 20 min at RT, and imaged on an Opera high-throughput imaging system. Control cells containing no peptide were treated with media only. Robust TRs between 3.5–4.0 were detected for Dex-treated cells under all plating densities and media tested. For $\mathbf{1}^{Dex}$ and $\mathbf{2}^{Dex}$, TRs were higher in transfection media (around 3.0 for both) compared to complete media (around 2.0 for both). For RNAi screening, 2,500 cells per well were plated in transfection medium, as these conditions resulted in a high number of cells per well (150–250 per image) without overcrowding and the highest TRs for Dex alone (TR = 3.4 ± 0.40), dex-peptide conjugates $\mathbf{1}^{Dex}$ (TR = 3.0 ± 0.40), and $\mathbf{2}^{Dex}$ (TR = 3.0 ± 0.090) (Fig. S5B).

Integration of Saos-2(GIGT) cells with High-Content RNAi Screening. High-Content RNAi screening was performed in 384-well format. To each well, siRNA duplex buffer (10 µL) with or without siRNA (20 nM), Opti-MEM (10 µL) containing Lipofectamine RNAiMAX (0.1 µL), and Saos-2(GIGT) cells (2500 per well) in complete McCoy's 5A medium without phenol red (30 µL per well, 10% FBS, without antibiotics) were added using a Multidrop Combi reagent dispenser (Thermo Scientific). The outer four columns of each 384-well plate contained experimental controls, while the inner 20 columns contained variable siRNAs, with four duplexes targeting a single gene within each well (SMARTpool siRNA). Background GR*eGFP translocation ratios (TRs) were determined from column 24, which contained untreated GR*eGFP cells transfected with non-targeting (RISC-Free) siRNA, while $\mathbf{1}^{Dex}$ TRs were represented in columns 2 and 23. Plate-wide transfection efficiency was determined from column 1, which contained alternating medium-only and Kif11 siRNA control wells. Knockdown of Kif11 results in mitotic arrest, phenotypically observable enlarged nuclei, and, ultimately, cell death (16). The significant loss in cell number upon Kif11 transfection, relative to RISC-Free transfection, is commonly used as a measure of siRNA transfection efficiency during high-throughput screens. In a pilot screen, we identified that siRNAs targeting the *SYNJ2BP* gene enhanced GR*eGFP translocation in the presence of $\mathbf{1}^{Dex}$ and yields a hit-like phenotype. We therefore included SYNJ2BP siRNA in columns 2 and 23 of every plate, to provide a representation of a hit candidate. Cells were reverse-transfected as follows: siRNA (20 nM) in sterile duplex buffer (10 µL) were first dispensed into each well, followed by Lipofectamine RNAiMAX (0.1 µL) in Opti-MEM (10 µL). After siRNAs and Lipofectamine RNAiMAX were allowed to complex for 20 min, Saos-2(GIGT) cells in McCoy's 5A without phenol red (30 µL, 10% FBS, without antibiotics) were dispensed into each well. Saos-2(GIGT) cells were allowed to settle for 30 min at RT, prior to placement into a 37 °C humidified incubator with 5% CO_2 for 56 h. After 56 h of reverse-transfection, cells were serum-starved for 16 h by replacing the media in each well with McCoy's 5A medium, without phenol red (30 µL, without FBS, without antibiotics).

High-Content Imaging of Saos-2(GIGT) Cells. After serum starvation, 10 µL clear McCoy's

5A medium supplemented with ligand at 5x concentration was overlaid onto wells, and Saos-2(GIGT) cells were incubated in the presence of Dex-peptide conjugates for 30 min. Following treatment, cells were fixed with 4% paraformaldehyde for 20 min at RT, washed twice with DPBS, stained with Hoechst 33342 (300 nM) for 45 min at RT, washed twice more, and imaged on an Opera high-throughput spinning disk confocal microscope.

Next, the reproducibility of GIGT assay was tested across two identical panels of 320 siRNAs targeting genes across the Dharmacon Human Genome Library. Non-treated Saos-2(GIGT) cells transfected with non-targeting siRNA displayed a mean TR of 1.2 ± 0.1 while identical cells treated with 1 μM $\mathbf{1}^{\text{Dex}}$ for 30 min displayed a mean TR of 2.4 ± 0.3. Across a panel of 320 test siRNAs, this system yielded a mean signal-to-background of 2.3, coefficient of variation (CV) of 11.2%, Z-factor of 0.30, and Pearson R correlation coefficient of 0.80 between two replicate plates (Fig. S5C). Collectively, these results underscore the adequacy of the GIGT system towards high-content RNAi screening.

Screening system: Opera (PerkinElmer Life and Analytical Sciences) using a 20x 0.45 NA lens. GR*-eGFP fluorescence was detected using a solid state 488 nm laser and a 540/75 band-pass filter, while Hoechst 33342 was detected using a 405 nm laser and a 450/50 band-pass filter. Three images were taken per well, and each image typically contained 200–300 cells. GR*-eGFP TRs were determined using Acapella high content imaging and analysis software (Perkin Elmer).

Plate Performance (Z-Factor Analysis). Individual plate performance was determined based on the Z-factor (Z′) between positive RISC-Free transfected Saos-2(GIGT) cells treated with 1 μM $\mathbf{1}^{\text{Dex}}$ and negative cells transfected with RISC-Free and left untreated, which was calculated using Equation 9:

$$Z' = 1 - \frac{3(\sigma_+ + \sigma_-)}{\mu_+ - \mu_-} \qquad \text{(Equation 9)}$$

Where μ_+ and σ_+ refer to the mean and standard deviation of Saos-2(GIGT) cells transfected with RISC-Free siRNA and treated with 1 μM $\mathbf{1}^{\text{Dex}}$, while μ_- and σ_- refer to the mean and standard deviation of nontreated cells transfected with RISC-Free non-targeting siRNA.

RNAi Translocation Data Normalization. Raw TRs were converted to normalized percent effect values using Equation 10. Data were normalized with respective controls per plate (17).

$$\text{Normalized \%-effect} = \frac{X_i - \mu_+}{\mu_+ - \mu_-} \cdot 100\% \qquad \text{(Equation 10)}$$

Where X_i is the mean GR*-eGFP TR of the respective RNAi knockdown, μ_+ is the mean TR of cells transfected with RISC-Free siRNA and treated with 1 μM $\mathbf{1}^{\text{Dex}}$ and μ_- is the mean TR of nontreated cells transfected with RISC-Free siRNA. The normalized %-effect of Saos-2(GIGT) cells transfected with RISC-Free siRNA and treated 1 μM $\mathbf{1}^{\text{Dex}}$ was defined as 0%, while that of nontreated Saos-2(GIGT) cells transfected with RISC-Free siRNA was defined as 100%.

Calculation of Z-Score. The Z-score, or the number of standard deviations between each knockdown and the mean TR of Saos-2(GIGT) cells transfected with RISC-Free siRNA and treated with 1 μM $\mathbf{1}^{\mathrm{Dex}}$ (μ_+), were calculated using Equation 11:

$$\text{Z-score} = \frac{\mu_+ - \mu_x}{\sigma_+} \qquad \text{(Equation 11)}$$

Where μ_+ is the mean TR of Saos-2(GIGT) cells transfected with RISC-Free siRNA and treated with 1 μM $\mathbf{1}^{\mathrm{Dex}}$, and σ_+ is the standard deviation of this population. μ_x refers to the mean TR of the respective RNAi knockdown.

RNAi Screen Hit Assignment Using Strictly Standardized Mean Difference (SSMD). To assign hits within the data set, normalized %-effect values from triplicate knockdowns were converted to strictly standardized mean difference (SSMD or β) values with Equation 12 (18):

$$\beta(\text{SSMD}) = \frac{\mu_+ - \mu_x}{\sqrt{\sigma_+^2 + \sigma_x^2}} \qquad \text{(Equation 12)}$$

Where μ_x is the mean %-effect of Saos-2(GIGT) cells transfected with gene-specific siRNAs and treated with 1 μM $\mathbf{1}^{\mathrm{Dex}}$ and σ_x refers to the standard deviation of this population. μ_+ and σ_+ refer to the mean %-effect of Saos-2(GIGT) cells transfected with RISC-Free siRNA and treated 1 μM $\mathbf{1}^{\mathrm{Dex}}$ and to the standard deviation of this population.

siRNA Reverse Transfection for Hit Validation by FC and FCS. This protocol was adapted from the manufacturer's protocol and optimized for 6-well plates. It was used for RT-qPCR, FC, and FCS experiments. Saos-2 cells (passage 5–20) were lifted with TrypLE Express for 10 min at 37 °C, 5% CO_2, and pelleted in complete McCoy's 5A medium without phenol red (15% FBS, 1 mM sodium pyruvate, without P/S) at 200 *g* for 3 min. Cells were resuspended in the same media and counted. For each well to be transfected, the appropriate amount of siRNA (100 nM final concentration, Table S3) was diluted in Opti-MEM (200 μL) and vortexed briefly to mix (solution A). In parallel, for each well to be transfected, Lipofectamine RNAiMAX (5 μL) was diluted in Opti-MEM (200 μL), and vortexed briefly to mix (solution B). Solutions A and B were mixed in a 1:1 ratio, vortexed briefly to mix, and incubated for 5 min at RT. To each well, Saos-2 cells (80,000 cells/well) were added in complete McCoy's 5A medium without phenol red (1.6 mL, 15% FBS, 1 mM sodium pyruvate, without P/S). The RNAi duplex-Lipofectamine RNAiMAX complexes (400 μL) were added dropwise to the cell solution in each well. Cells were mixed gently by rocking the 6-well plate back and forth (final volume of medium/well = 2 mL). Cells were moved to the incubator (37 °C, 5% CO_2). After 3.5 h, Saos-2 cells were washed three times with pre-warmed DPBS (4 mL/well, 3 min/wash) to remove Lipofectamine RNAiMAX. Media was replaced with fresh complete growth medium without phenol red (2 mL/well, 15% FBS, 1 mM sodium pyruvate, without antibiotics). Saos-2 cells were incubated for 72 h at 37 °C, 5% CO_2 for optimal gene knockdown. Control cells were transfected with Lipofectamine RNAiMAX only, or with a non-targeting siRNA (RISC-Free) and Lipofectamine RNAiMAX. To assess

transfection efficiency, Kif11 siRNA was used. Knockdown of Kif11 leads to mitotic arrest and cell death. This phenotype was used as a visual control for transfection efficiency.

Confirming Knockdown by RT-qPCR. Saos-2 cells were reverse-transfected in 6-well plates as described above. Total RNA was extracted using the RNeasy Mini kit (Qiagen, #74104), 48 or 72 h after transfection. RNA was reverse-transribed with Superscript III reverse transcriptase (Thermo Fisher Scientific) and gene-specific primers (IDT, PrimeTime qPCR primers, Table S3) according to the manufacturer's protocol. For RT-qPCR, cDNA was amplified with SsoFast EvaGreen Supermix (Bio-Rad, Hercules, CA, USA) on a Bio-Rad CFX96 real-time PCR detection system. Each biological replicate was run in triplicate, assayed for the siRNA-targeted gene and compared to GAPDH serving as an endogenous reference gene (Fig. S6A).

FC and FCS to Quantify Cytosolic Access. Saos-2 cells were reverse-transfected in 6-well plates as described above. The next day, the medium was removed and cells were washed twice with DPBS. Cells were incubated with peptides $\mathbf{1}^{R}$–$\mathbf{5}^{R}$ (600 nM) in clear McCoy's 5A medium without phenol red (1 mL/well, without FBS, without sodium pyruvate, without P/S) for 30 min at 37 °C, 5% CO_2. While cells were incubating, an 8-well microscopy slide (Thermo Scientific, #155411) was coated with fibronectin from bovine plasma in DPBS (1:100 dilution, 200 µL/well) for 1 h at 37 °C (200 µL/well). The fibronectin solution was removed by aspiration and the dish was washed three times with DPBS before use. Nuclei were labeled with Hoechst 33342 (300 nM) for 5 min at the end of the 30-min incubation period by adding the nuclear stain to the peptide-containing medium. To remove exogenously bound peptide, cells were washed three times with DBPS and treated with TrypLE Express (500 µL/well) for 10 min until all cells were lifted from the culture dish. Cells were transferred to 15-mL Falcon tubes, each well was rinsed twice with complete McCoy's 5A medium without phenol red (twice, 1 mL each), and the cell suspensions, including media used for rinsing, were pooled and pelleted at 200 *g* for 3 min. The supernatant was removed and cells were resuspended in HEPES-containing clear DMEM without phenol red (1 mL, 25 mM HEPES, without FBS, without sodium pyruvate, without P/S) to wash the pellet. Cells were pelleted again at 200 *g* for 3 min. The supernatant was removed and cells were resuspended in HEPES-containing clear DMEM without phenol red (600 µL). Of this suspension, one third (200 µL) was plated into the prepared fibronectin-coated microscopy dish and cells were left to adhere at 37 °C, 5% CO_2 for at least 20 min before FCS experiments were performed. The remaining two thirds of the cell suspension were pelleted again at 200 *g* for 3 min, resuspended in DPBS (200 µL) and transferred to a polystyrene round bottom 96-well plate (#353077, Falcon) for flow cytometry analysis. Flow cytometry was performed on a BD Accuri C6 Flow Cytometer (excitation laser: 488 nm, emission filter: 585 ± 40 nm) or on an Attune NxT flow cytometer (excitation laser: 561 nm, emission filter: 585 ± 16 nm) at RT. At least 10,000 cells were analyzed for each sample. FCS experiments were performed as described above. Flow cytometry data was analyzed using FlowJo software (version 7.6.1, FlowJo, LLC).

HOPS Activity Assay Using Alexa 488 Dextran and Magic Red. Magic Red is a fluorogenic substrate for the lysosomal hydrolase cathepsin B (19). It becomes fluorescent in the presence of active cathepsin B—an enzyme exclusively localized to mature lysosomes. For the first experiment, displayed in Fig. S9A–C, Saos-2 cells were transfected with siRNAs targeting

VPS39 or VPS41 72 h before the assay was performed. For the second experiment, displayed in Fig. S9D–F, Saos-2 cells were plated in tissue culture-treated 6-well plates (100,000 cells/well) in complete McCoy's 5A medium without phenol red (2 mL/well, 15% FBS, 1 mM sodium pyruvate, without P/S) 18 h before the assay was performed. After 18 or 72 h, respectively, the medium was removed and cells were washed twice with DPBS. Cells were incubated with 0.5 mg/mL dextran Alexa Fluor 488 10,000 MW, anionic, fixable (Life Technologies) in clear McCoy's 5A medium without phenol red (1 mL/well, without FBS, without sodium pyruvate, without P/S) for 2 h at 37 °C, 5% CO_2 followed by a 1-h chase period in dextran-free McCoy's 5A medium. While cells were incubating, an 8-well microscopy slide (Thermo Scientific, #155411) was coated with fibronectin from bovine plasma in DPBS (1:100 dilution, 200 µL/well) for 1 h at 37 °C (200 µL/well). The fibronectin solution was removed by aspiration and the dish was washed three times with DPBS before use. During the hour-long chase period, cells were rinsed three times with DPBS and nuclei were stained with Hoechst 33342 (300 nM) for 5 min. To remove exogenously bound dextran, cells were then washed three times with DBPS and treated with TrypLE Express (500 µL/well) for 10 min until all cells were lifted from the culture dish. Cells were transferred to 15-mL Falcon tubes, each well was rinsed twice with complete McCoy's 5A without phenol red (1 mL each), and the cell suspensions, including media used for rinsing, were pooled and pelleted at 200 *g* for 3 min. The supernatant was removed and cells were re-suspended in 1 mL HEPES-containing clear DMEM without phenol red (25 mM HEPES, without FBS, without sodium pyruvate, without P/S) to wash the pellet. Of this suspension, half (300 µL) was plated into the prepared fibronectin-coated microscopy dish. Cells were left to adhere at 37 °C, 5% CO_2 for the remainder of the hour-long chase period at 37 °C, 5% CO_2. Cells were then incubated in a 1:2600 dilution of Magic Red Cathepsin B substrate (ImmunoChemistry Technologies, #937) in clear DMEM without phenol red for 5 min at 37 °C, 5% CO_2. Cell images were recorded on an LSM 880 microscope. The degree of colocalization of two channels reflecting the fraction of dextran Alexa Fluor 488 colocalizing with Magic Red was measured by Pearson correlation coefficient (20) using ImageJ software (version 1.48s, NIH).

Multi-Color Confocal Fluorescence Microscopy. *With siRNA knockdown* (Fig. 5): Saos-2 cells were transfected with siRNAs targeting VPS39 or TGFBRAP, or a non-targeting siRNA (RISC-Free) 72 h (day –3) prior to the experiment. *Without siRNA knockdown* (Fig. 4, S11, S12): Saos-2 cells were plated in tissue culture-treated 6-well plates (100,000 cells/well) in complete McCoy's 5A medium without phenol red (2 mL/well, 15% FBS, 1 mM sodium pyruvate, without P/S) 48 h (day –2) prior to the experiment. On day –1, cells were transduced with CellLight early endosomes, late endosomes, or lysosomes-GFP (BacMam 2.0, Life Technologies, #C10586, #C10588, #C10596) according to the manufacturer's protocol. On day 0 (= 18 h after transduction), the media were removed and cells were washed twice with DPBS. Cells were incubated with or without *N*-Rh-PE (16:0 Liss Rhod PE, Avanti Polar Lipids, #81058) in clear McCoy's 5A without phenol red (1 mL/well, without FBS, without sodium pyruvate, without P/S) for 1 h at 4 °C. Cells were washed with DPBS three times and incubated with CPMP $\mathbf{2}^{R}$ (300 nM) or $\mathbf{2}^{SiR}$ (600 nM) in clear McCoy's 5A media without phenol red for 30 min at 37 °C, 5% CO_2. While cells were incubating, an 8-well microscopy slide (Thermo Scientific, #155411) was coated with fibronectin from bovine plasma in DPBS (1:100 dilution, 200 µL/well) for 1 h at 37 °C (200 µL/well). The fibronectin solution was removed by aspiration and the dish was washed

three times with DPBS before use. After the 30-min incubation period with CPMP **2**, nuclei were stained with Hoechst 33342 (300 nM) for 5 min at 37 °C, 5% CO_2. To remove exogenously bound CPMPs, cells were washed three times with DBPS and treated with TrypLE Express (500 µL/well) for 10 min until all cells were lifted from the culture dish. Cells were transferred to 15-mL Falcon tubes, each well from the tissue culture dish was rinsed twice with complete McCoy's 5A media without phenol red (twice, 1 mL each), and the cell suspensions including media used for rinsing were combined and pelleted at 200 *g* for 3 min. The supernatant was removed and cells were resuspended in HEPES-containing clear DMEM without phenol red (1 mL, 25 mM HEPES, without FBS, without sodium pyruvate, without P/S) to wash the pellet. Of this suspension, half (300 µL) was plated into the prepared fibronectin-coated microscopy dish. To enlarge $Rab7^+$-endosomes, Saos-2 cells were incubated with YM201636 (800 nM) in clear DMEM without phenol red for 1 h at 37 °C, 5% CO_2. Cell images were recorded on an LSM 880 microscope (Zeiss) using the following imaging settings: Hoechst excitation: 405 nm (Diode 405-30 laser) and emission: 410–496 nm. eGFP excitation: 488 nm (Argon laser), emission: 490–526 nm. Lissamine RhoB excitation: 561 nm (DPSS 561-10 laser), emission: 570–607 nm. Silicon rhodamine excitation: 633 nm (HeNe633 laser), emission 650–747 nm. The degree of colocalization of two channels was measured by Pearson *r* correlation coefficient (20) using ImageJ software (version 1.48s, NIH).

Quantification and Statistical Analysis

All the data were presented as mean ± standard error from at least three independent trials. All data fitting and statistical analysis was performed using GraphPad Prism software (version 7.0a).

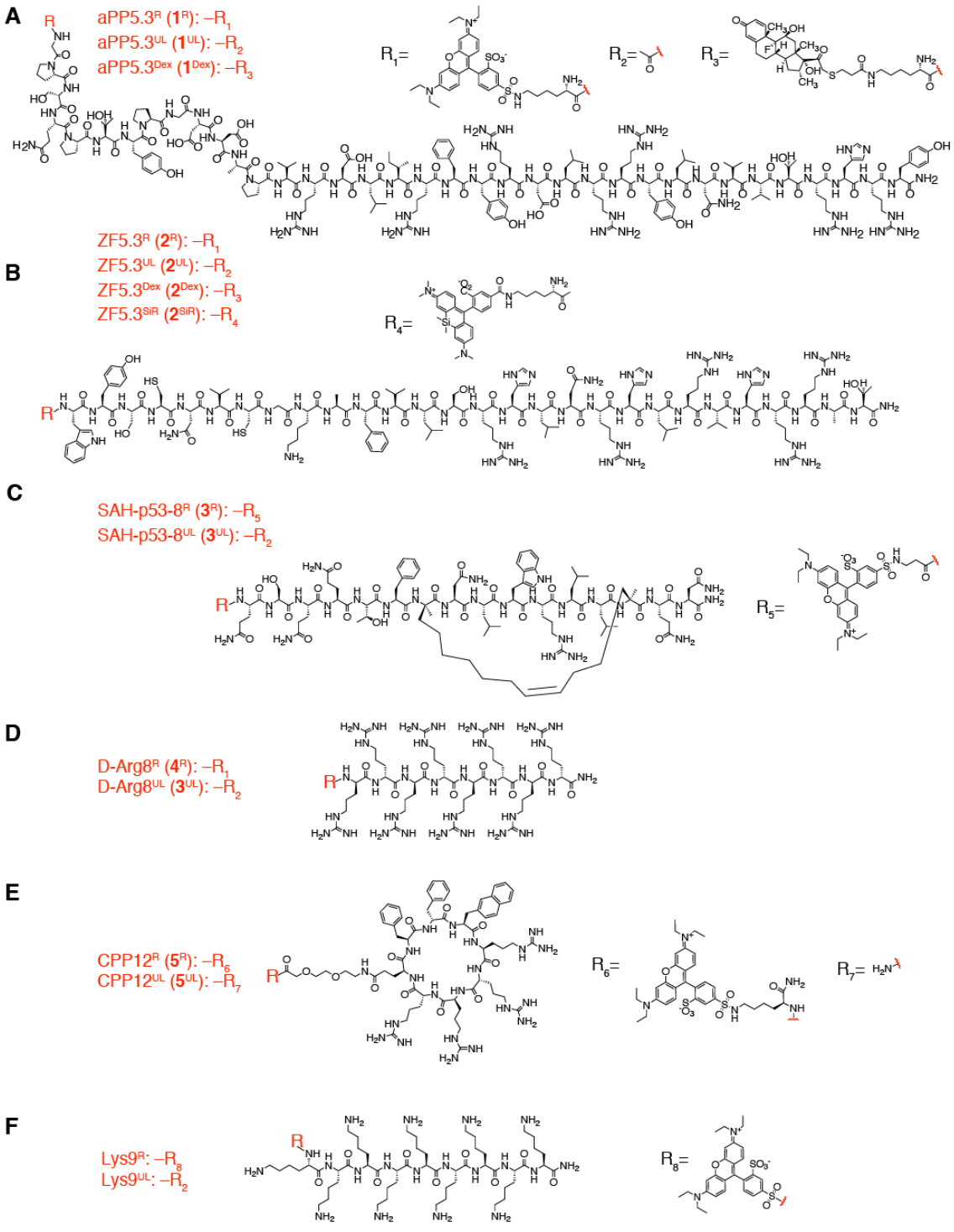

Fig. S1. Structures of CPMP and CPP variants.

Structures of unlabeled (UL), Lissamine Rhodamine B (R)-labeled, dexamethasone (Dex)-tagged,

and silicon rhodamine (SiR)-labeled variants off CPMPs and CPPs studied in this work. (A) aPP5.3 (**1**) variants; (B) ZF5.3 (**2**) variants; (C) SAH-p53-8 (**3**) variants; (D) D-Arg8 (**4**) variants; (E) CPP12 (**5**) variants; (F) Lys9 variants. Note: for $\mathbf{1}^{R}$, $\mathbf{2}^{R}$, $\mathbf{4}^{R}$, and $\mathbf{5}^{R}$, the RhoB-tag was attached to a lysine side chain, while in $\mathbf{3}^{R}$, the RhoB-tag was appended to β-alanine at the N-terminus. $Lys9^{R}$ was labeled with RhoB at the N-terminus.

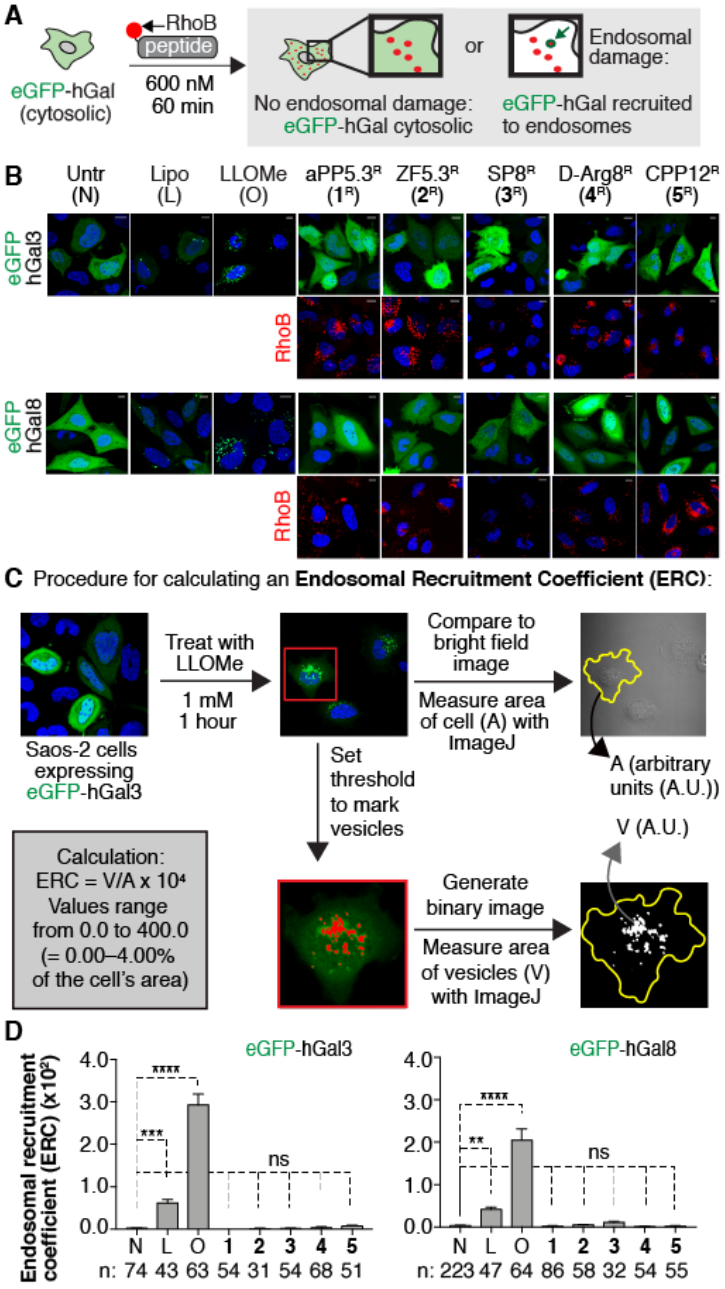

Fig. S2. CPMPs/CPPs induce little or no galectin recruitment at 600 nM.

(A) Experimental scheme. Saos-2 cells transiently expressing eGFP fusions of human galectins 3 and 8 (eGFP-hGal3 or eGFP-hGal8) were treated with 600 nM of the indicated lissamine rhodamine B (RhoB)-labeled CPMP or CPP (**1**^{R}–**5**^{R}) for 60 min. This incubation was followed by a 30-min chase in CPP/CPMP-free culture media and visualization of the cells using confocal microscopy. Cells lacking endosomal damage exhibit diffuse cytosolic fluorescence due to cytosolic eGFP-hGal3 or eGFP-hGal8. Cells with endosomal damage exhibit punctate fluorescence indicating hGal recruitment by cytosolically displayed β-galactosides on endosomal membranes. (B and D) Representative live-cell confocal fluorescence microscopy images of Saos-2 cells expressing eGFP-hGal3 or eGFP-hGal8 incubated with McCoy's 5A media only

(Untr, N), Lipofectamine RNAiMAX (16 µL/mL) (Lipo, L), LLOMe (1 mM) (O), or Rho-tagged CPMPs/CPPs $\mathbf{1}^{R}$–$\mathbf{5}^{R}$ at 600 nM. Nuclei were stained with Hoechst 33342. Top rows: green channel detecting eGFP-hGals. Bottom rows: red channel detecting RhoB-tagged CPMPs/CPPs. (C) Procedure for calculating an endosomal recruitment coefficient (ERC). In the example shown, Saos-2 cells expressing eGFP-hGal3 were treated with LLOMe (1 mM) for 1 hour to induce endolysosomal damage. Before LLOMe treatment, cells displayed diffuse cytosolic eGFP-hGal3 fluorescence. After LLOMe treatment, the eGFP-hGal3 fluorescence became predominantly punctate. To calculate the ERC, we measured the area (A) of each cell in the bright field channel using ImageJ. Second, we manually set a threshold to mark vesicular structures and generated a binary image thereof. Third, we measured the area of the punctate vesicles (V). Lastly, the ERC was calculated as the ratio of V over A multiplied by a factor of 10^4. We routinely obtained ERC values around 0.0 in untreated cells and 400.0 in LLOMe-treated cells, which corresponds to 0% and 4% vesicular staining compared to the total cell area. (D) ERCs were calculated for n cells and error bars represent the standard error of the mean. ****$p < 0.0001$, ***$p < 0.001$, **$p < 0.01$, *$p < 0.05$ and not significant (ns) for $p > 0.05$ from one-way ANOVA with Dunnett post-test. Scale bars = 10 µm.

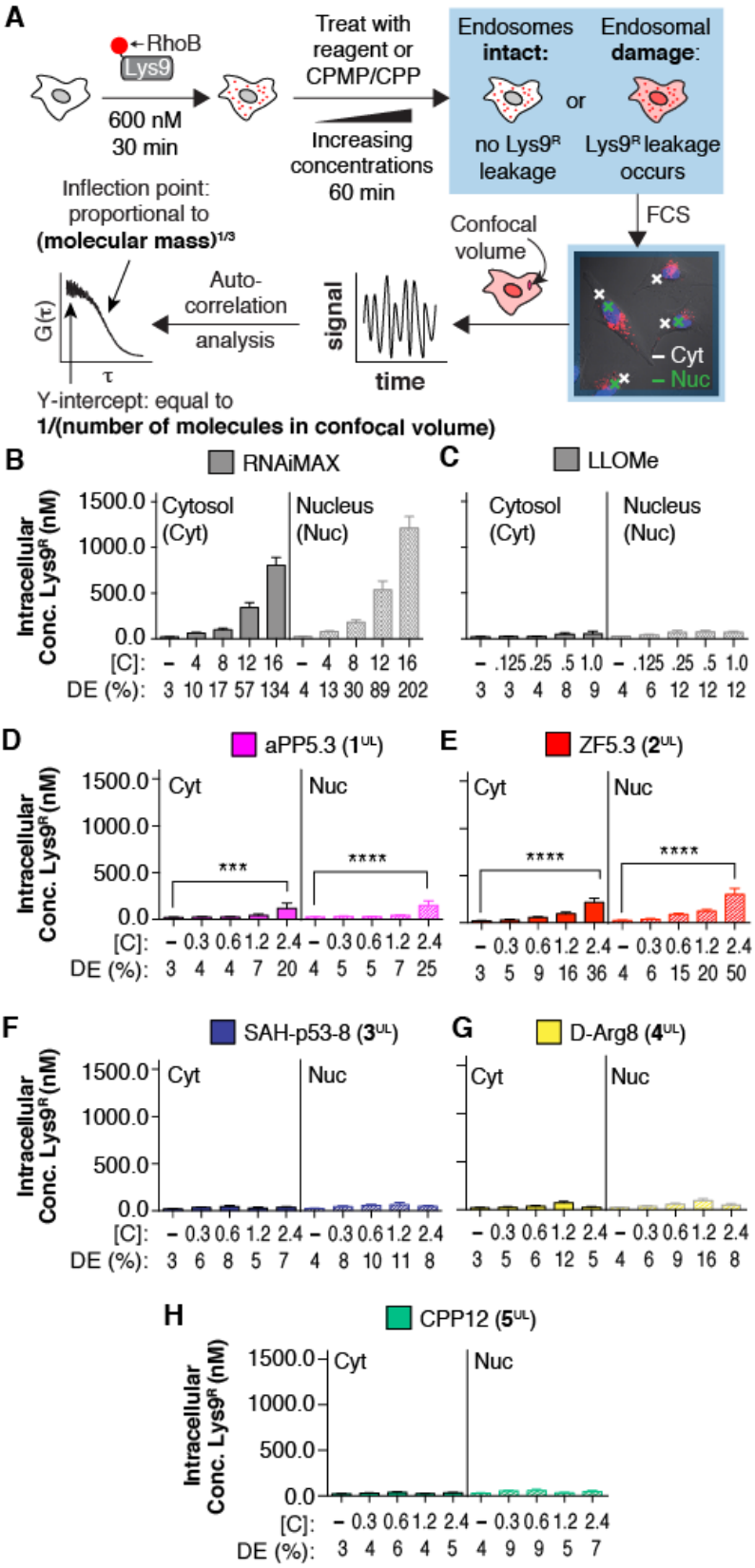
A
RhoB
Lys9
600 nM
30 min
Treat with reagent or CPMP/CPP
Increasing concentrations
60 min
Endosomes intact:
no Lys9R leakage
or
Endosomal damage:
Lys9R leakage occurs
FCS
Confocal volume
– Cyt
– Nuc
signal
time
Auto-correlation analysis
G(τ)
τ
Inflection point: proportional to (molecular mass)1/3
Y-intercept: equal to 1/(number of molecules in confocal volume)
B
RNAiMAX
C
LLOMe
Intracellular Conc. Lys9R (nM)
Cytosol (Cyt)
Nucleus (Nuc)
[C]:
DE (%):
D
aPP5.3 (1UL)
E
ZF5.3 (2UL)
F
SAH-p53-8 (3UL)
G
D-Arg8 (4UL)
H
CPP12 (5UL)
Cyt
Nuc
***
****

Fig. S3. CPMPs/CPPs do not induce endosomal leakage at concentrations below 2 µM.

(A) Experimental scheme. Saos-2 cells were treated with $Lys9^R$ (600 nM) for 30 minutes, washed extensively, and treated with either Lipofectamine RNAiMAX (0, 4, 8, 12, 16 µL/mL), LLOMe (0, 0.125, 0.25, 0.5, 1.0 mM) or with CPMP or CPP $\mathbf{1}^{UL}$–$\mathbf{5}^{UL}$ (0.3, 0.6, 1.2, 2.4 µM) for 60 minutes. The concentration of $Lys9^R$ in the cytosol and nucleus was determined using FCS. Cells whose endosomes remain intact are characterized by low concentrations of $Lys9^R$ in the cytosol and nucleus, whereas cells whose endosomes have released some or all of their contents are characterized by higher levels of $Lys9^R$ in the cytosol and nucleus. FCS data were obtained using a commercial Zeiss LSM 880 microscope. Images of cells were acquired in the x–y plane, and the laser's crosshair (= confocal volume) was placed in the nucleus or cytosol of cells, avoiding areas with high, punctate endosomal signal. Fluorescent fluctuations over time were recorded on a GaAsP detector and traces were converted to autocorrelation curves using a custom MATLAB script. Individual autocorrelation traces were averaged prior to fitting to a 3D diffusion model containing parameters for anomalous diffusion and background autocorrelation as described in LaRochelle et al., 2015. The fitted data points were assessed individually and filtered for data quality by evaluating diffusion time (τ), signal intensity, and the anomalous diffusion coefficient (α). The inflection point of the autocorrelation fit is proportional to the cubic root of the molecular mass. The y-intercept equals the inverse of the number of molecules in the confocal volume. For more details, see methods section. (B–G) Intracellular $Lys9^R$ concentration in the cytosol (Cyt) or nucleus (Nuc) of $Lys9^R$-pretreated Saos-2 cells incubated with Lipofectamine RNAiMAX ([C] = 0, 4, 8, 12, 16 µL/mL), LLOMe ([C] = 0, 0.125, 0.25, 0.5, 1.0 mM) or CPMPs/CPPs $\mathbf{1}^{UL}$–$\mathbf{5}^{UL}$ ([C] = 0.3, 0.6, 1.2, 2.4 µM). Intracellular $Lys9^R$ concentrations were calculated for $n > 10$ cells. The delivery efficiency (DE) is the ratio of the measured intracellular (Cyt or Nuc) $Lys9^R$ concentration to the $Lys9^R$ incubation concentration (600 nM) multiplied by 100%. Error bars represent the standard error of the mean. ****$p < 0.0001$, ***$p < 0.001$, and not significant (ns) for $p > 0.05$ from one-way ANOVA with Dunnett post-test.

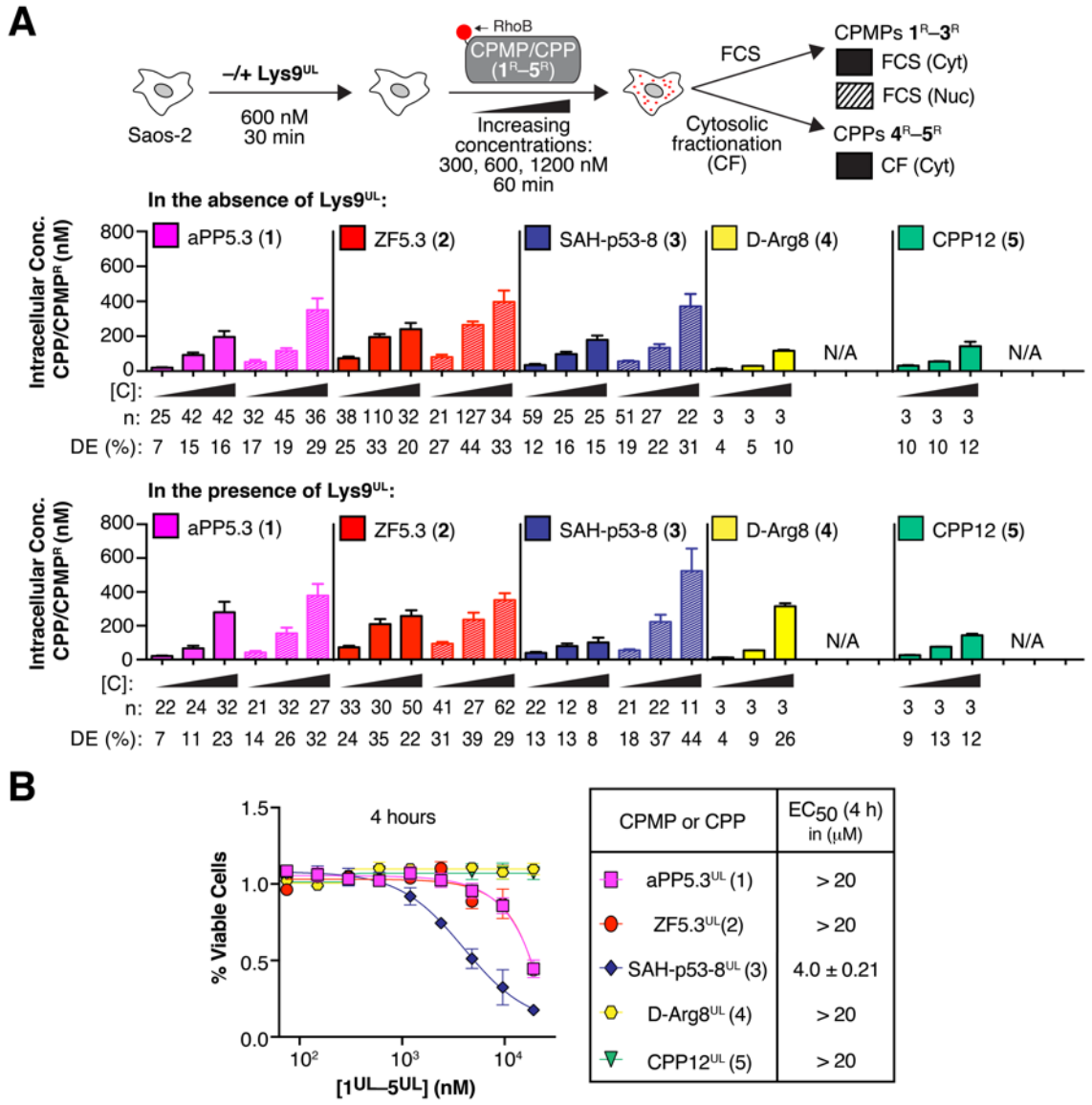

Fig. S4. Control experiments to support and accompany Figure S3.

(A) To investigate the effects of Lys9 on the intracellular delivery of peptides **1**–**5**, we incubated Saos-2 cells that had been pre-treated with or without unlabeled Lys9 (Lys9^{UL}) (600 nM) with lissamine rhodamine B (RhoB)-tagged CPMPs/CPPs **1**^{R}–**5**^{R} (300, 600, and 1200 nM), and quantified intracellular delivery of **1**^{R}–**3**^{R} *via* FCS and of **4**^{R} and **5**^{R} *via* fractionation. We were unable to perform FCS experiments at CPMP/CPP concentrations above 1200 nM because the concentration of fluorescent molecules in the confocal volume was too high—especially for CPMP **2**^{R} and hydrocarbon-stapled peptide **3**^{R}—to obtain satisfactory fits to their corresponding autocorrelation curves. For FCS, concentrations were calculated for n cells in the cytosol (Cyt) and nucleus (Nuc) and error bars represent the standard error of the mean. For fractionation, concentrations were calculated for n biological replicates of 1.5 x 10^{6} homogenized cells and normalized to an equal population of cells treated with **2**^{R} at the same concentration. The

cytosolic concentration of $\mathbf{2}^{R}$ is known because it was measured using FCS. For fractionation, nuclear concentrations are not available (N/A). The delivery efficiency (DE) is the ratio of the measured intracellular (Cyt or Nuc) $Lys9^{R}$ concentration to the $Lys9^{R}$ incubation concentration (600 nM) multiplied by 100%. (B) Effect of CPPs/CPMPs $\mathbf{1}^{R}$–$\mathbf{5}^{R}$ on cell proliferation. Plot of % viable cells remaining after 4 h treatment with [molecule] shown. Viability was assessed by monitoring oxyluciferin production by Ultra-Glow luciferase, a reaction that requires ATP. Error bars show standard error of the mean. EC_{50} values in μM.

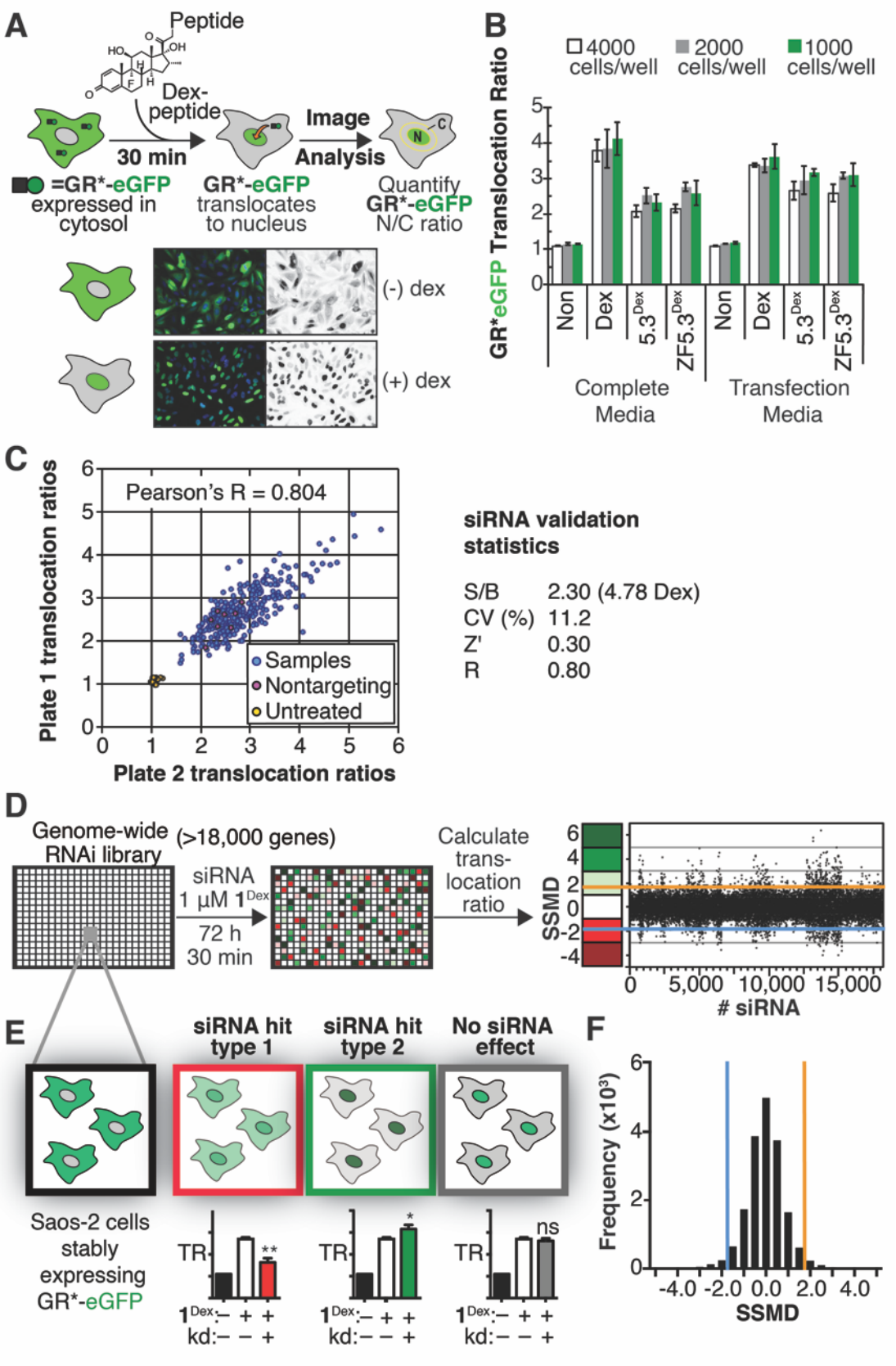
A
Peptide
Dex-peptide
30 min
Image Analysis
=GR*-eGFP expressed in cytosol
GR*-eGFP translocates to nucleus
Quantify GR*-eGFP N/C ratio
(-) dex
(+) dex
B
4000 cells/well
2000 cells/well
1000 cells/well
GR*eGFP Translocation Ratio
Non
Dex
5.3Dex
ZF5.3Dex
Complete Media
Transfection Media
C
Pearson's R = 0.804
Plate 1 translocation ratios
Plate 2 translocation ratios
Samples
Nontargeting
Untreated
siRNA validation statistics
S/B 2.30 (4.78 Dex)
CV (%) 11.2
Z' 0.30
R 0.80
D
Genome-wide RNAi library (>18,000 genes)
siRNA 1 µM 1Dex
72 h 30 min
Calculate trans-location ratio
SSMD
siRNA
E
siRNA hit type 1
siRNA hit type 2
No siRNA effect
Saos-2 cells stably expressing GR*-eGFP
TR
1Dex
kd:
ns
F
Frequency (x10³)
SSMD

Fig. S5. Genome-wide high content RNAi screen identifies genes involved in CPMP trafficking to cytosol.

(A) Overview of the glucocorticoid-induced eGFP translocation (GIGT) assay. Saos-2 cells stably expressing GR(C638G)-eGFP (= GR*-eGFP) were treated with dexamethasone (Dex) or a Dex-labeled peptide to induce the nuclear translocation of GR*-eGFP. The extent of nuclear translocation was quantified by a translocation ratio (TR), defined as the ratio of the nuclear to cytoplasmic (N/C) signal due to GR*-eGFP as determined using fluorescence microscopy and high content image analysis software (CellProfiler35 and Acapella). (B) Optimization of seeding density and RNAi growth medium in Saos-2(GIGT) cells. Saos-2(GIGT) cells were plated at various seeding densities in either complete growth medium (McCoy's 5A, with pen/strep, 15% FBS) or transfection medium (complete growth medium/Opti-MEM/RNAi duplex buffer, 3:1:1). After 72 h, cells were treated with DMEM containing either 1 μM Dex or a CPMP-Dex conjugate ($\mathbf{1}^{Dex}$ or $\mathbf{2}^{Dex}$) for 30 min, after which cells were fixed with paraformaldehyde, stained with Hoechst 33342, and imaged on an Opera High Content Screening System. Control cells (Non) were treated with media only. The RNAi screen was performed using 2,500 cells per well plated in transfection medium, as these conditions resulted in a high number of cells per well without overcrowding and resulted in the highest TRs for Dex alone. (C) Reproducibility of an RNAi pilot screen of 320 randomly chosen, duplicate siRNAs from the Dharmacon Human siGENOME siRNA Library (SMARTpool). Across this siRNA test panel, the GIGT system yielded a mean signal-to-background ratio of 2.3, coefficient of variation (CV) of 11.2%, Z-factor (Z') of 0.3, and Pearson's correlation coefficient (R) of 0.8. (D) Genome-wide RNAi screen. We screened the Dharmacon human siGENOME siRNA library (>18,000 genes) in Saos-2 cells stably expressing GR(C638G)-eGFP (GR*-eGFP) to identify genes whose knockdown lead to significant changes in the cytosolic trafficking of CPMP $\mathbf{1}^{Dex}$. Cytosolic localization was monitored using the GIGT assay (Holub et al., 2013) where the reporter translocation ratio (TR) refers to the ratio of the median GFP signal in the nucleus to the median signal within a 2-μm annulus of cytosol that surrounds the nucleus (Appelbaum et al., 2012). Saos-2(GIGT) cells were transfected with pools of four siRNAs (in triplicate) for 72 hours, serum-starved, and then treated with $\mathbf{1}^{Dex}$ (1 μM) for 30 minutes. The cells were fixed, stained with Hoechst 33342, and imaged on an Opera High Content Screening System. Raw TR values associated with each well were normalized to percent effect values, relative to control cells transfected with non-targeting siRNA and treated with $\mathbf{1}^{Dex}$. We identified 428 primary hits based on the strictly standardized mean difference (β = SSMD) (Zhang et al., 2007) threshold of ±2.0. (E) Candidate genes whose knockdown inhibited the cytosolic access of $\mathbf{1}^{Dex}$ were defined by low TRs relative to control cells treated with non-targeting siRNA and $\mathbf{1}^{Dex}$ (siRNA hit type 1); candidate genes whose knockdown enhanced the cytosolic access of $\mathbf{1}^{Dex}$ were defined by high TRs relative to control cells (siRNA hit type 2); candidate genes whose knockdown led to no significant TR changes in the ability of $\mathbf{1}^{Dex}$ to reach the cytosol were excluded from further analyses (no siRNA effect). (F) An SSMD cutoff of ±2.0 resulted in an overall hit rate of 2.4%.

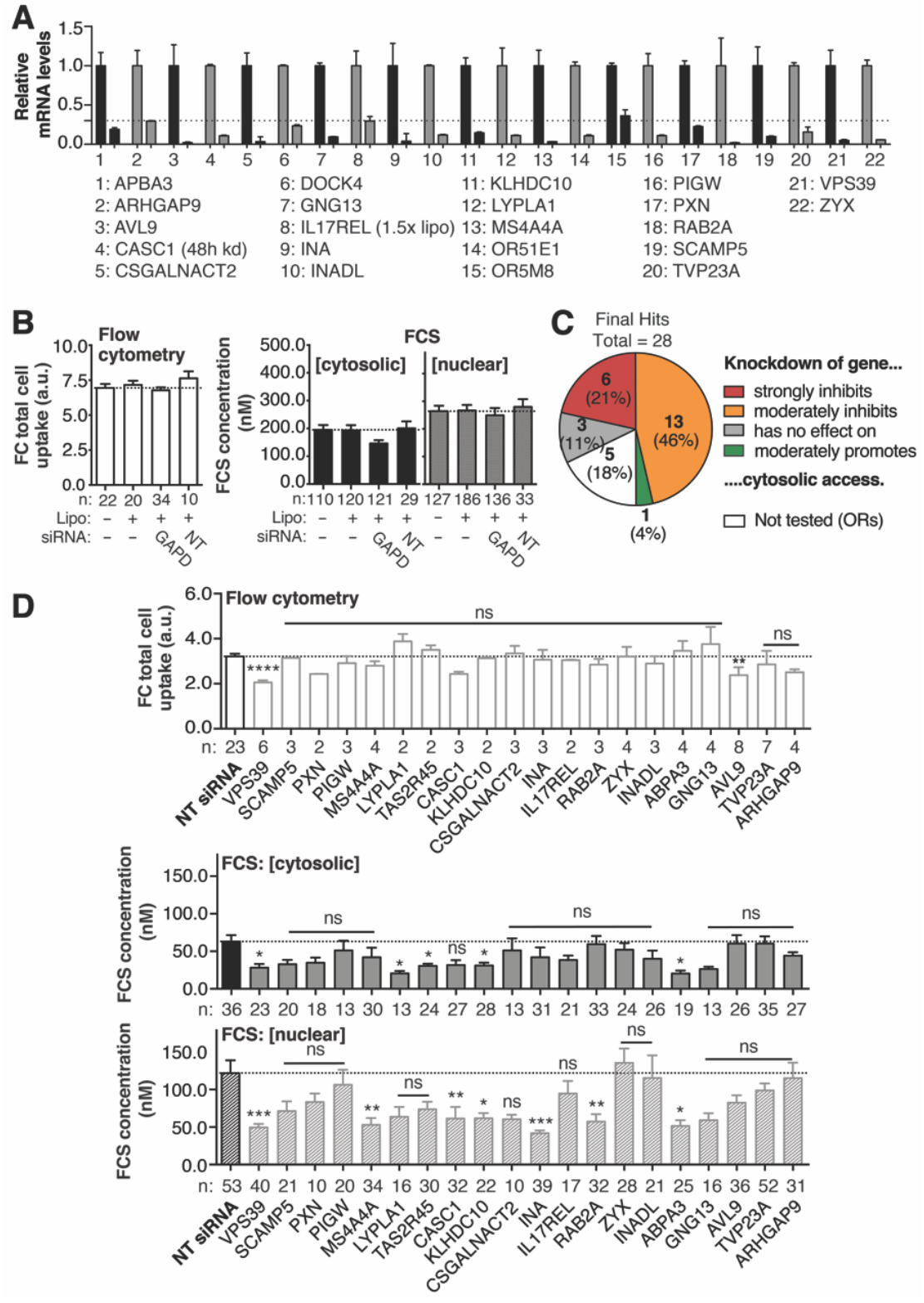

Fig. S6. Supplementary figures to support and accompany Figure 2.

(A) RT-qPCR to confirm gene knockdown: Saos-2 cells were transfected with Lipofectamine RNAiMAX and siGENOME SMARTpool siRNAs (Dharmacon). Total RNA was extracted 72 h

(unless noted otherwise) after transfection. RNA was reverse-transcribed with gene-specific primers according to the manufacturer's protocol. For RT-qPCR, cDNA was amplified using SsoFast EvaGreen Supermix assay. Each biological replicate was run in triplicate, and assayed for both the siRNA-targeted gene and GAPDH (endogenous reference gene). (B) Negative transfection controls for FC and FCS. Saos-2 cells were transfected with siGENOME SMARTpool siRNAs (Dharmacon) for 72 hours according to the manufacturer's protocol. Cells were treated with CPMP $\mathbf{2}^{R}$ (600 nM) for 30 minutes and exogenously bound peptide was removed with TrypLE Express. Whole-cell fluorescence intensities were measured by FC and cytosolic and nuclear concentrations were measured by FCS in untreated (without Lipofectamine RNAiMAX, without siRNA) cells, in cells treated with Lipofectamine RNAiMAX, in cells treated with Lipofectamine RNAiMAX and a non-targeting (RISC-Free) siRNA, and in cells treated with Lipofectamine RNAiMAX and an siRNA against the *GAPD* housekeeping gene. No significant differences were detected among all controls. (C) Of the 28 final hits identified in the GIGT high-throughput screen, knockdown of six genes strongly inhibited cytosolic access, knockdown of 13 genes moderately inhibited cytosolic access, knockdown of one gene promoted cytosolic access, and knockdown of three genes had no effect on cytosolic access (false positives). The remaining five genes, which were classified as false positives, belong to a group of seven olfactory receptors (ORs), which exhibit high sequence homology (>40%) among each other. Two representative ORs were tested and displayed no significant effects compared to NT siRNA. (D) Effects of validated genes on the delivery of $\mathbf{3}^{R}$: Saos-2 cells were transfected with siRNAs targeting the 20 validated genes identified in Figure 3 and then treated with hydrocarbon-stapled peptide $\mathbf{3}^{R}$ (600 nM). FC and FCS effects were compared to non-targeting (NT, RISC-Free) siRNA-transfected cells. FC: total cell uptake, fluorescence intensity at 585 nm. Each data point (n) represents one biological replicate. For each FC replicate, the median fluorescence intensity at 585 nm was measured for at least 10,000 Saos-2 cells (gated for live cells). FCS: cytosolic and nuclear concentration (nM). Each data point (n) represents a 50-second FCS measurement recorded in a single cell. Error bars represent the standard error of the mean. ****$p < 0.0001$, ***$p < 0.001$, **$p < 0.01$, *$p < 0.05$, and not significant (ns) for $p > 0.05$ from one-way ANOVA with Dunnett post-test.

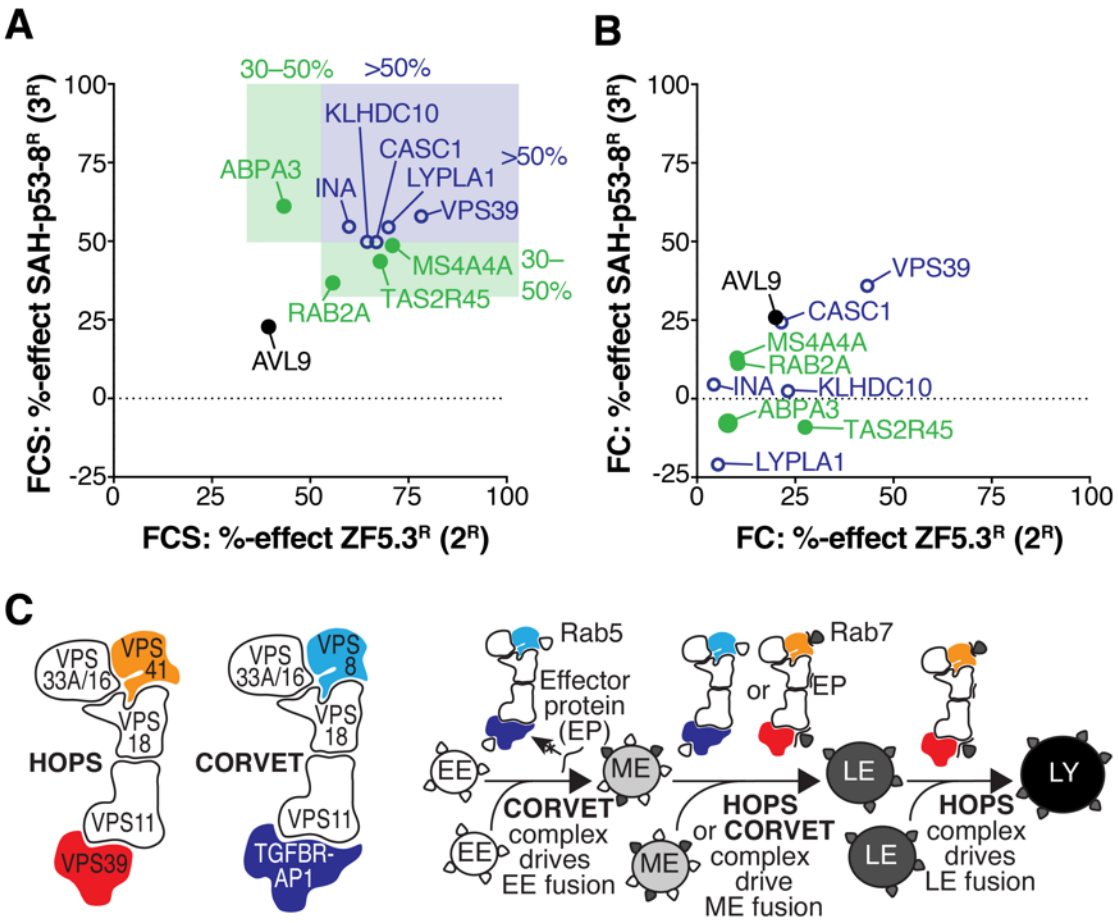

Fig. S7. Comparison of the effects of gene-specific knockdown on uptake and cytosolic trafficking of CPMP 2 and hydrocarbon-stapled peptide 3.

(A) Comparison of the effects of gene-specific knockdowns on the cytosolic trafficking of CPMP **2**^{R} and hydrocarbon stapled peptide **3**^{R} as determined by FCS. Graph includes only those genes with significant (by one-way ANOVA with Dunnett post-test) FCS effects for both **2**^{R} and **3**^{R}. The %-effect for each siRNA knockdown was calculated by dividing the average intracellular concentration ($C_{nucleus}$ + $C_{Cytosol}$ divided by two) measured by FCS in gene-specific siRNA-transfected cells by the average intracellular concentration measured in cells transfected with a non-targeting siRNA (RISC-Free), multiplied by 100%. (B) Comparison of the effects of gene-specific knockdowns (same genes as in (A)) on the cytosolic trafficking of CPMP **2**^{R} and hydrocarbon stapled peptide **3**^{R} as determined by flow cytometry (FC). The %-effect for each siRNA knockdown was calculated by dividing the average overall uptake fluorescence intensity measured by FC in gene-specific siRNA-transfected cells by the average overall uptake fluorescence intensity measured in cells transfected with a non-targeting siRNA (RISC-Free), multiplied by 100%. (C) The strongest identified gene hit for both **2**^{R} and **3**R—*VPS39*—encodes a subunit of the human HOPS membrane tethering complex, which is closely related to the human CORVET complex. (B) CORVET and HOPS initiate endosomal contact and fusion along the degradative endocytic pathway. CORVET drives the fusion of Rab5^{+} early endosomes (EEs) and maturing endosomes (MEs), while HOPS drives fusion of Rab7^{+} MEs and late endosomes

(LEs) to form lysosomes (LYs).

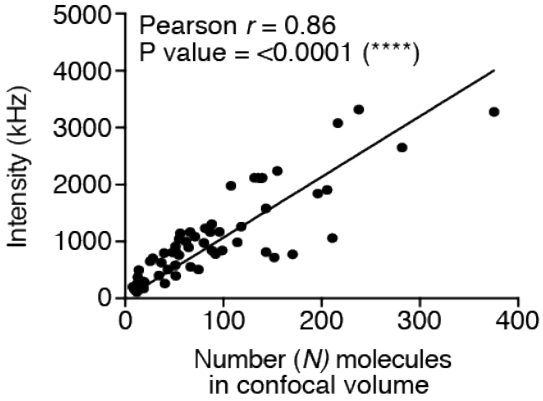

Fig. S8. FCS intensity is proportional to the number of molecules in the confocal volume. The FCS intensity (in kHz) is proportional to the number (*N*) of molecules detected in the confocal volume for a laser. Each data point represents one 50-second FCS measurement recorded in the nucleus or cytosol of a single Saos-2 cell treated with $\mathbf{2}^{R}$ (600 nM) for 30 min.

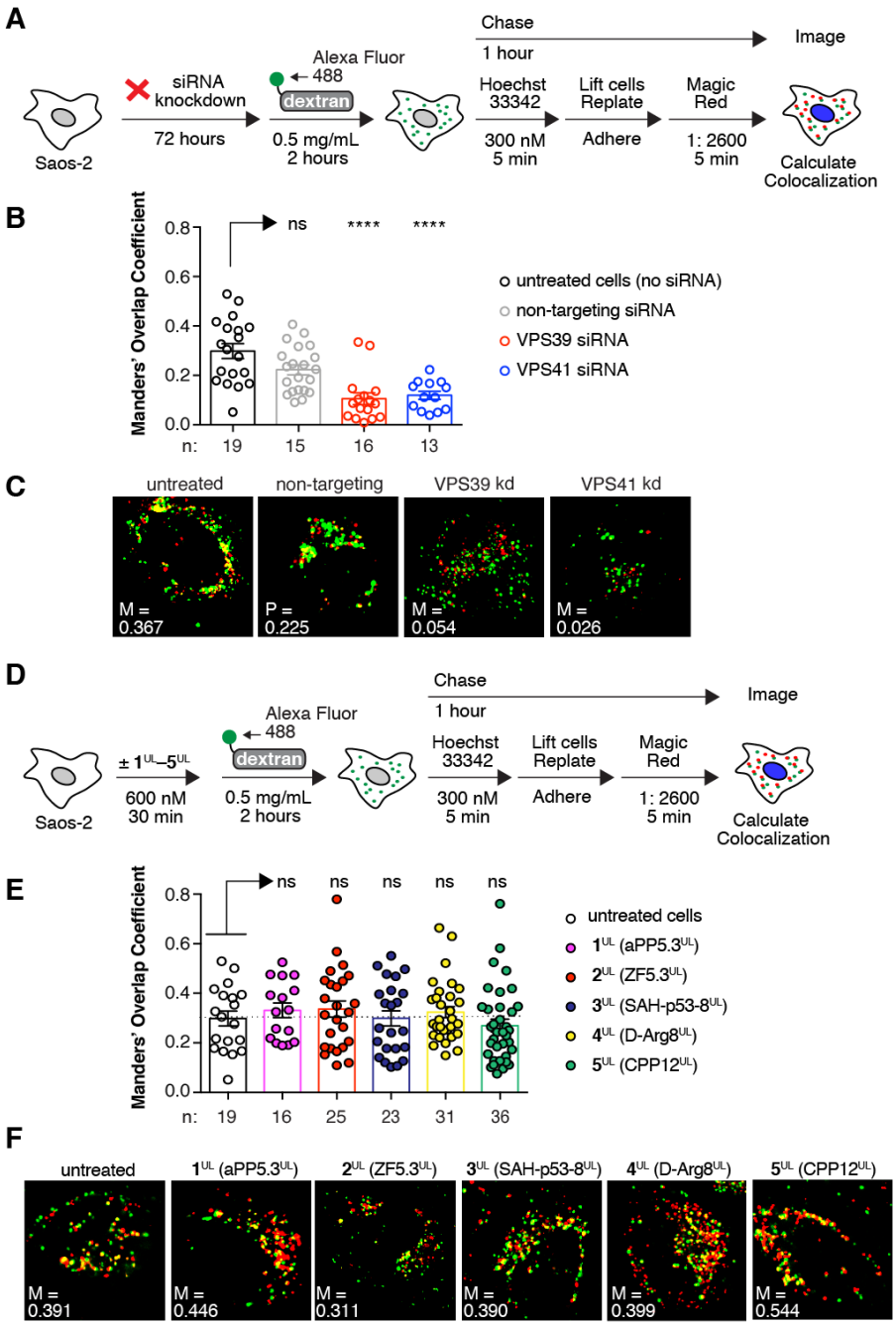

Fig. S9. HOPS activity studies.

(A) Saos-2 cells were transfected with Lipofectamine RNAiMAX and siGENOME SMARTpool siRNAs (Dharmacon) targeting VPS39 or VPS41. After 72 h, cells were incubated with Alexa Fluor 488-tagged dextran (10,000 MW, anionic, fixable) for 2 h. Cells were washed, nuclei were stained with Hoechst 33342, cells were replated, and lysosomes were stained with Magic Red for 5 min. (B) Colocalization of Alexa Fluor 488-tagged dextran with Magic Red (Manders M2) in live-cell confocal microscopy images after knockdown of HOPS proteins VPS39 and VPS41 with SMARTpool siRNA compared to a non-targeting (RISC-Free) RNA. Error bars represent the

standard error of the mean. ****$p < 0.0001$ from one-way ANOVA with Dunnett post-test. (C) Representative live-cell confocal microscopy images of cells quantified in (B). (D) Saos-2 cells were treated with CPMPs/CPPs $\mathbf{1}^{UL}$–$\mathbf{5}^{UL}$. After 30 min, the media was replaced and cells were incubated with Alexa Fluor 488-tagged dextran for 2 h. Cells were washed, nuclei were stained with Hoechst 33342, cells were replated, and lysosomes were stained with Magic Red dye for 5 min. (E) Colocalization of Alexa Fluor 488-tagged dextran with Magic Red (Manders M2) in live-cell confocal microscopy images after treatment with CPMPs/CPPs $\mathbf{1}^{UL}$–$\mathbf{5}^{UL}$ for 30 min at 37 °C, 5% CO_2. Error bars represent the standard error of the mean. Not significant (ns) for $p > 0.05$ from one-way ANOVA with Dunnett post-test. (F) Representative live-cell confocal microscopy images of cells quantified in (E).

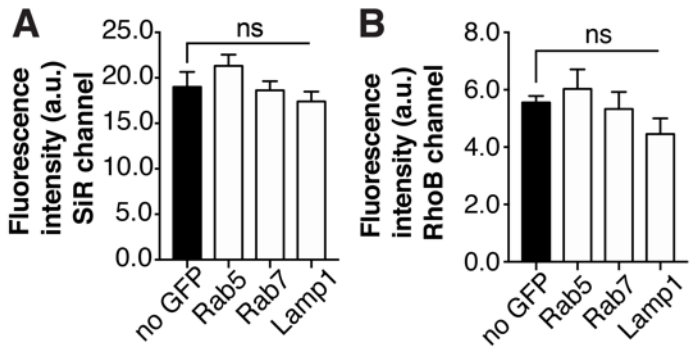

Fig. S10 Effect of GFP overexpression on CPMP 2 overall uptake.
(A and B) Fluorescence intensity of Saos-2 cells treated with $\mathbf{2}^{R}$ (300 nM) (A) or $\mathbf{2}^{SiR}$ (600 nM) (B) expressing either no GFP-tagged protein (no GFP), Rab5-, Rab7-, or Lamp1-GFP, as measured by flow cytometry (FC). Each bar consists of at least three biological replicates. For each FC replicate, the median fluorescence intensity at 585 nm was measured for at least 10,000 Saos-2 cells (gated for live cells). Error bars represent the standard error of the mean. Not significant (ns) for $p > 0.05$ from one-way ANOVA with Dunnett post-test.

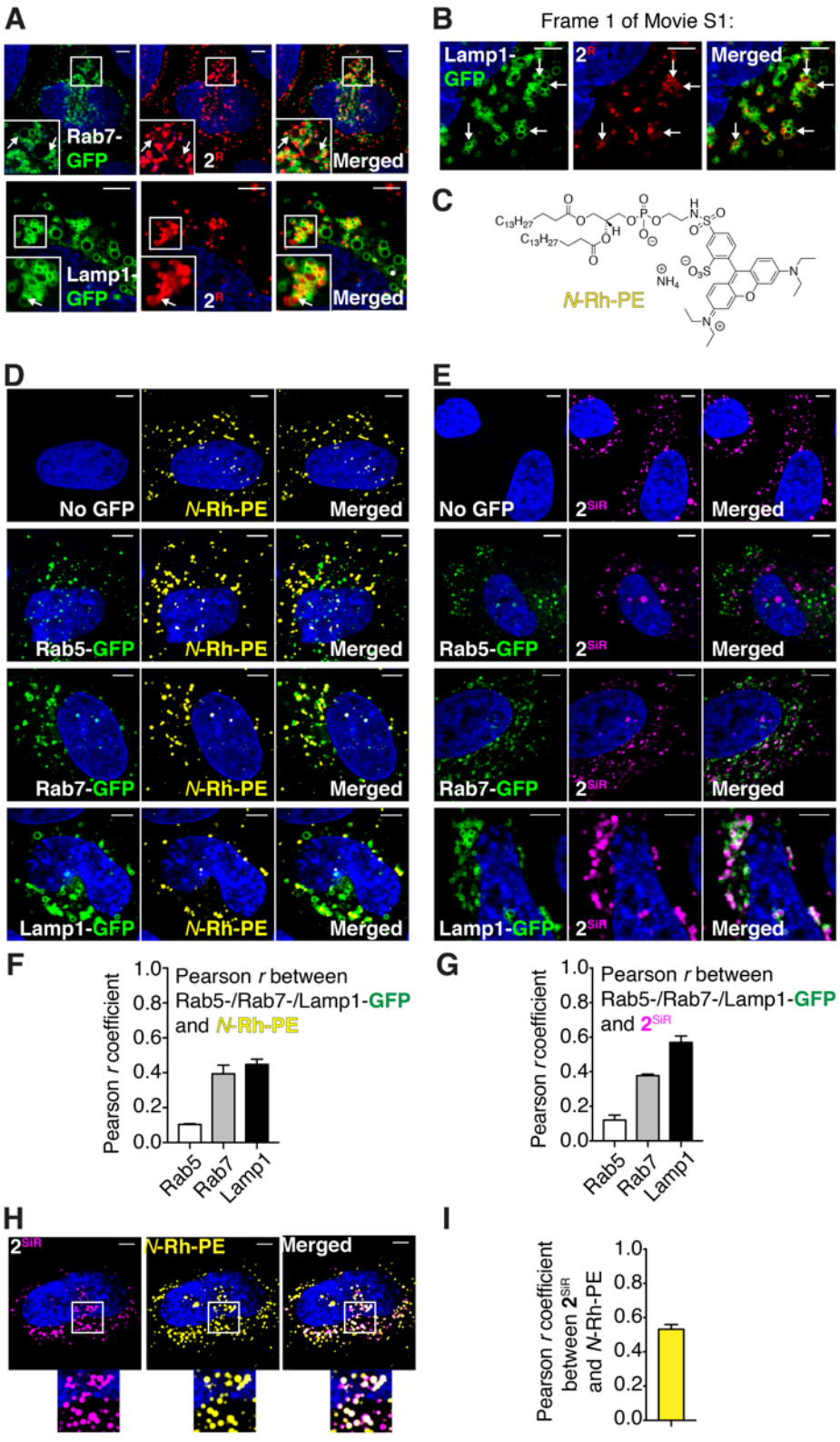

Fig. S11. CPMP 2 localizes to the lumen of LEs and LYs. (A) Saos-2 cells were transduced with Rab7- or Lamp1-GFP for 18 hours using CellLight Reagents (BacMam 2.0). Cells were

washed, incubated with CPMP $\mathbf{2}^{R}$ (300 nM), stained with Hoechst 33342, lifted with TrypLE, and re-plated into microscopy slides. Cells were then incubated in media containing YM201636 (800 nM) for 1 hour. White arrows identify smaller vesicles present within the boundaries of Rab7-GFP^{+} or Lamp1-GFP^{+} endosomes. (B) Representative live-cell confocal fluorescence image of the first frame of Movie S1. White arrows identify Lamp1-GFP^{+} endosomes that contain moving vesicles labeled with CPMP $\mathbf{2}^{R}$ (+YM201636), as shown in Movies S1 and S2. (C) Structure of ILV marker lipid *N*-Rh-PE. (D) Representative live-cell confococal microscopy images of Saos-2 cells transduced with Rab5-, Rab7-, or Lamp1-GFP for 18 h using CellLight Reagents (BacMam 2.0). Cells were washed and incubated with *N*-Rh-PE for 1 h at 4 °C. (E) Representative live-cell confocal microscopy images of Saos-2 cells transduced with Rab5-, Rab7-, or Lamp1-GFP for 18 h using CellLight Reagents (BacMam 2.0). Cells were washed and incubated with $\mathbf{2}^{SiR}$ (600 nM) for 30 min. (F and G) Pearson correlation coefficients between GFP markers and *N*-Rh-PE (F), and GFP markers and $\mathbf{2}^{SiR}$ (G). (H) Representative live-cell confocal microscopy images of Saos-2 cells treated with CPMP $\mathbf{2}^{SiR}$ and ILV marker *N*-Rh-PE. (I) Pearson correlation coefficient between $\mathbf{2}^{SiR}$ and ILV marker *N*-Rh-PE. Scale bars = 5 μm.

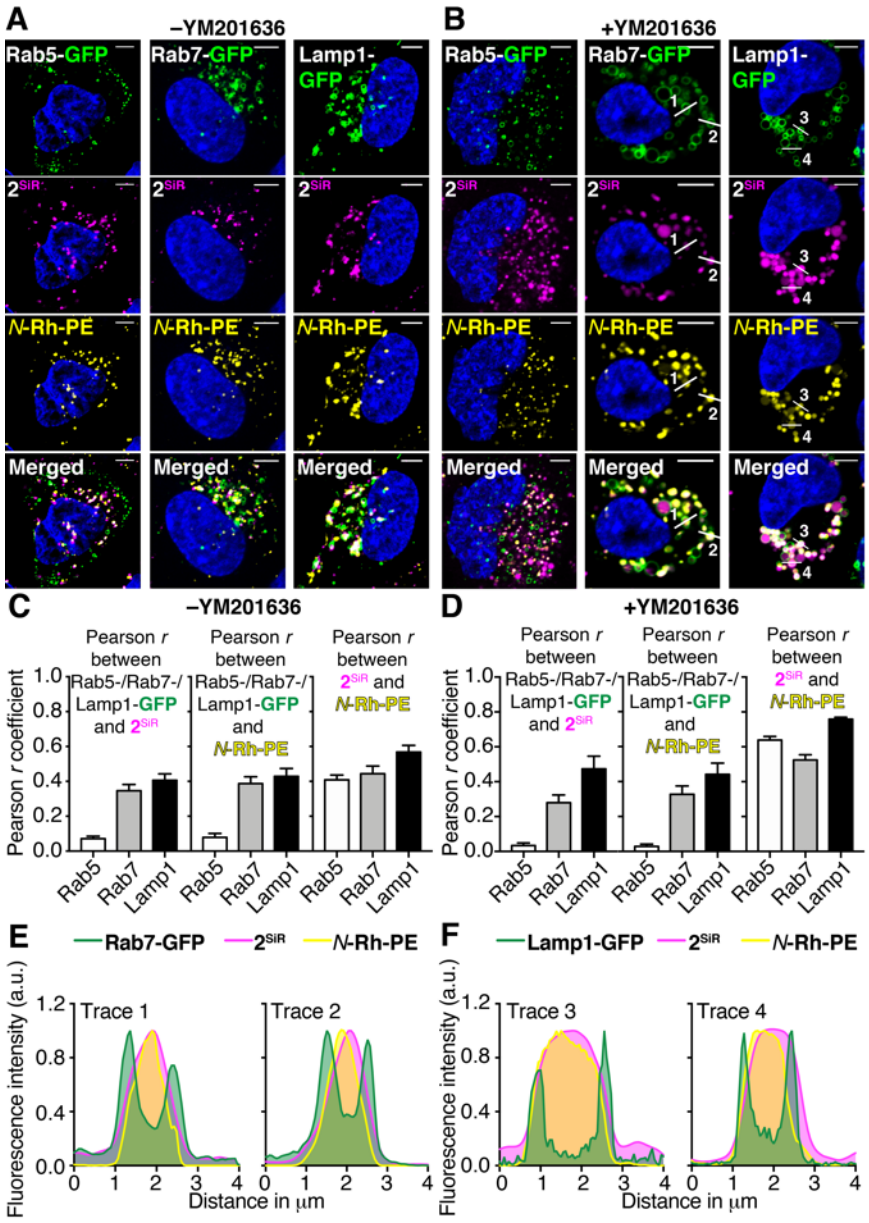

Fig. S12. CPMP 2 colocalizes with ILV marker *N*-Rh-PE.

CPMP 2 localizes to ILVs in LEs and LYs. Saos-2 cells were transduced with Rab5-, Rab7-, or Lamp1-GFP for 18 h using CellLight Reagents (BacMam 2.0). To label ILVs, cells were incubated with *N*-Rh-PE (5 μM) for 1 h at 4 °C. Cells were washed and incubated with CPMP 2^{SiR} (600 nM) for 30 min and nuclei were stained with Hoechst 33342 (300 nM) for 5 min. Cells were trypsinized and re-plated into microscopy slides, after which they were incubated in media with or without YM201636 (800 nM) for 1 hour. (A and B) Representative live-cell confocal fluorescence microscopy images of Saos-2 cells incubated without YM201636 (A) or with YM201636 (B) present. (C and D) Pearson correlation coefficients between pairs of specified markers without YM201636 (C) or with YM201636 (D) present. (E and F) Fluorescence intensity line profiles of endosomes (#1–4, see panel C) generated in ImageJ. Scale bars = 5 μm.

Table S1. Sequences, calculated & observed exact masses of all CPMP and CPP variants.

CPMP/CPP	Sequence	Exact mass $[M+H]^+$ calc.	Exact mass $[M+H]^+$ found
aPP5.3^{UL} (**1**^{UL})	Ac-GPSQPTYPGDDAPVRDLIRFYRDLRRYLN VVTRHRY-$CONH_2$	4403.30	4403.18
aPP5.3^{R} (**1**^{R})	K^{RhoB}-GPSQPTYPGDDAPVRDLIRFYRDLRRYLN VVTRHRY-$CONH_2$	5029.53	5029.28
aPP5.3^{Dex} (**1**^{Dex})	K^{Dex}-GPSQPTYPGDDAPVRDLIRFYRDLRRYLN VVTRHRY-$CONH_2$	4951.57	4951.41
ZF5.3^{UL} (**2**^{UL})	Ac-WYSCNVCGKAFVLSRHLNRHLRVHRRAT -$CONH_2$	3420.80	3420.82
ZF5.3^{R} (**2**^{R})	K^{RhoB}-WYSCNVCGKAFVLSRHLNRHLRVHRRAT -$CONH_2$	4047.03	4047.01
ZF5.3^{SiR} (**2**^{SiR})	K^{SiR}-WYSCNVCGKAFVLSRHLNRHLRVHRRAT -$CONH_2$	3961.06	3960.82
ZF5.3^{Dex} (**2**^{Dex})	K^{Dex}-WYSCNVCGKAFVLSRHLNRHLRVHRRAT -$CONH_2$	3969.07	3968.11
SAH-p53-8^{UL} (**3**^{UL})	Ac-QSQQTFR_8NLWRLLS_5QN-$CONH_2$	2109.16	2109.15
SAH-p53-8^{R} (**3**^{R})	^{RhoB}βA-QSQQTFR_8NLWRLLS_5QN-$CONH_2$	2678.33	2678.23
D-Arg8^{UL} (**4**^{UL})	Ac-rrrrrrrr-$CONH_2$	Purchased (Genscript)	
D-Arg8^{R} (**4**^{R})	K^{RhoB}-rrrrrrrr-$CONH_2$	1935.08	1935.41
CPP12^{UL} (**5**^{UL})	miniPEG-cyclo(FfΦRrRrQ)-$CONH_2$	1389.77	1389.75
CPP12^{R} (**5**^{R})	K^{RhoB}-miniPEG-cyclo(FfΦRrRrQ)-$CONH_2$	2058.00	2057.91
Lys9^{UL}	Ac-KKKKKKKKK-$CONH_2$	Purchased (Genscript)	
Lys9^{R}	RhoB-KKKKKKKKK-$CONH_2$	1711.03	1711.00

Table S2. FCS diffusion parameters. Molecular weight, predicted and measured diffusion coefficients (*D*) either *in buffer only* and or *in the cytosol and nucleus* of Saos-2 cells treated with RhoB-tagged CPMP and CPP variants. The dimensions of the confocal volume were determined using Alexa Fluor 594 hydrazide (Life Technologies, #A10438), serving as an internal standard, as described above on page 7. The diffusion coefficient of Alexa Fluor 594 (100 nM) was measured in Milli-Q water at 37 °C. All other diffusion coefficients were measured in serum-free DMEM without phenol red (25 mM HEPES, pH 7.2) at 37 °C. For more details, see page 7.

	Molecular weight	**Predicted *D*** at 37 °C in $\mu m^2\ s^{-1}$	**Measured D** at 37 °C in $\mu m^2\ s^{-1}$	**Average *D*** in cytosol at 37 °C in $\mu m^2\ s^{-1}$	**Average *D*** in nucleus at 37 °C in $\mu m^2\ s^{-1}$
Alexa Fluor 594	758.79	520	520 (standard)	N/A	N/A
Lissamine RhoB-COOH	542.66	604	516 ± 5	N/A	N/A
aPP5.3^R (**1**^{R})	5031.77	278	231 ± 2	71 ± 13	86 ± 7.1
ZF5.3^R (**2**^{R})	4048.80	298	262 ± 3	88 ± 10	82 + 10
SAH-p53-8^R (**3**^{R})	2679.16	342	323 ± 2	35 ± 10	57 ± 21
D-Arg8^R (**4**^{R})	1935.37	382	306 ± 1	3.3 ± 0.24	4.4 ± 0.37
CPP12^R (**5**^{R})	2058.46	374	318 ± 2	3.1 ± 0.18	3.9 ± 0.29

Table S3. siRNAs and RT-qPCR primers.

Oligonucleotides	Supplier	Catalogue number
Human siGENOME siRNA Library – Genome – SMARTpool	Dharmacon	G-005005
siGENOME RISC-Free Control siRNA	Dharmacon	D-001220-01
siGENOME human GAPD Control siRNA	Dharmacon	D-001140-01
siGENOME human SMARTpool siRNA KIF11	Dharmacon	D-001220-01
siGENOME human SMARTpool siRNA APBA3	Dharmacon	M-011962-01
siGENOME human SMARTpool siRNA ARHGAP9	Dharmacon	M-010047-02
siGENOME human SMARTpool siRNA AVL9	Dharmacon	M-025311-01
siGENOME human SMARTpool siRNA CASC1	Dharmacon	M-027150-01
siGENOME human SMARTpool siRNA CSGALNACT2	Dharmacon	M-015941-00
siGENOME human SMARTpool siRNA DOCK4	Dharmacon	M-017968-01
siGENOME human SMARTpool siRNA GNG13	Dharmacon	M-020691-01
siGENOME human SMARTpool siRNA IL17REL	Dharmacon	M-033104-00
siGENOME human SMARTpool siRNA INA	Dharmacon	M-014975-00
siGENOME human SMARTpool siRNA KLHDC10	Dharmacon	M-025495-01
siGENOME human SMARTpool siRNA LYPLA1	Dharmacon	M-010007-01
siGENOME human SMARTpool siRNA MS4A4A	Dharmacon	M-017214-00
siGENOME human SMARTpool siRNA OR51E1	Dharmacon	M-003978-02
siGENOME human SMARTpool siRNA OR5M8	Dharmacon	M-032441-00
siGENOME human SMARTpool siRNA PATJ	Dharmacon	M-012112-01
siGENOME human SMARTpool siRNA PIGW	Dharmacon	M-021480-01
siGENOME human SMARTpool siRNA PXN	Dharmacon	M-005163-00
siGENOME human SMARTpool siRNA RAB2A	Dharmacon	M-010533-01
siGENOME human SMARTpool siRNA SCAMP5	Dharmacon	M-016650-0
siGENOME human SMARTpool siRNA TAS2R45	Dharmacon	M-017805-00
siGENOME human SMARTpool siRNA TGFBRAP1	Dharmacon	M-006903-01
siGENOME human SMARTpool siRNA TVP23A	Dharmacon	M-184329-01
siGENOME human SMARTpool siRNA VPS8	Dharmacon	M-023668-02
siGENOME human SMARTpool siRNA VPS39	Dharmacon	M-014052-01
siGENOME human SMARTpool siRNA VPS41	Dharmacon	M-006972-01
siGENOME human SMARTpool siRNA ZYX	Dharmacon	M-016734-01
GAPDH forward qPCR primer: 5'-TGCACCACCAACTGCTTAGC-3'	IDT	N/A
GAPDH reverse qPCR primer: 5'-GGCATGGACTGTGGTCATGAG-3'	IDT	N/A
PrimeTime qPCR primers ARHGAP9	IDT	Hs.PT.58.23217362.g
PrimeTime qPCR primers AVL9	IDT	Hs.PT.58.2309735
PrimeTime qPCR primers CASC1	IDT	Hs.PT.58.40973950
PrimeTime qPCR primers CSGALNACT2	IDT	Hs.PT.58.1381705
PrimeTime qPCR primers DOCK4	IDT	Hs.PT.58.4940825
PrimeTime qPCR primers GNG13	IDT	Hs.PT.58.38439062
PrimeTime qPCR primers IL17REL	IDT	Hs.PT.58.25111300
PrimeTime qPCR primers INA	IDT	Hs.PT.58.27216293

PrimeTime qPCR primers KLHDC10	IDT	Hs.PT.58.172069
PrimeTime qPCR primers LYPLA1	IDT	Hs.PT.58.38630572
PrimeTime qPCR primers MS4A4A	IDT	Hs.PT.58.22520387
PrimeTime qPCR primers OR51E1	IDT	Hs.PT.58.28309762
PrimeTime qPCR primers OR5M8	IDT	Hs.PT.58.24795111.g
PrimeTime qPCR primers INADL (PATJ)	IDT	Hs.PT.58.2857750
PrimeTime qPCR primers PIGW	IDT	Hs.PT.58.21355249
PrimeTime qPCR primers PXN	IDT	Hs.PT.58.25546662
PrimeTime qPCR primers RAB2A	IDT	Hs.PT.58.19561586
PrimeTime qPCR primers SCAMP5	IDT	Hs.PT.58.24622089
PrimeTime qPCR primers TGFBRAP1	IDT	Hs.PT.58.138528
PrimeTime qPCR primers TVP23A	IDT	Hs.PT.58.14454882
PrimeTime qPCR primers VPS8	IDT	Hs.PT.58.1611351
PrimeTime qPCR primers VPS39	IDT	Hs.PT.58.26949378
PrimeTime qPCR primers VPS41	IDT	Hs.PT.58.39633303
PrimeTime qPCR primers ZYX	IDT	Hs.PT.58.20549955
gBlock human galectin-8 (hGal) gene fragment	IDT	–

Movie S1. Single-color movie of ILV movement in Lamp1$^+$ endosomes. Saos-2 cells were transduced with Lamp1-GFP for 18 h using CellLight Reagents (BacMam 2.0). Cells were washed and incubated with CPMP **2**^{R} (300 nM) for 30 min and nuclei were stained with Hoechst 33342 (300 nM) for 5 min. Cells were lifted with TrypLE Express and re-plated into microscopy slides. Cells were incubated in media containing YM201636 (800 nM) for 1 hour. The GFP, RhoB, and Hoechst channels corresponding to the first frame of this movie can be found in Fig. S11B.

Movie S2. Dual-color movie of ILV movement in Lamp1$^+$ endosomes. Saos-2 cells were transduced with Lamp1-GFP for 18 h using CellLight Reagents (BacMam 2.0). Cells were washed and incubated with CPMP **2**^{R} (300 nM) for 30 min and nuclei were stained with Hoechst 33342 (300 nM) for 5 min. Cells were lifted with TrypLE Express and re-plated into microscopy slides. Cells were incubated in media containing YM201636 (800 nM) for 1 hour.

Dataset S1. Primary hits (428) of the GIGT siRNA screen. By setting an SSMD (see equation 12) threshold of ±2.0, we identified 263 genes whose knockdown enhance and 165 genes whose knockdown inhibit cytosolic access of CPMP **1**^{Dex}.

Dataset S2. Prioritized hits (131) of the GIGT siRNA screen. Of the 428 primary hits, we prioritized genes according to function. We retained genes with known roles in endocytic trafficking and genes with unknown or poorly characterized functions.

Dataset S3. Raw data of the GR*-eGFP translocation screen. During this filtering step, we retained a gene if its knockdown did not induce a significant change in the translocation ratio (TR) for at least two of the four gene-specific siRNAs (A–D) compared to cells transfected with a non-targeting (RISC-Free) siRNA. This process eliminated 61 of 131 genes with 70 genes remaining for follow-up analysis. ****$p < 0.0001$, ***$p < 0.001$, **$p < 0.01$, *$p < 0.05$, and not significant (ns) for $p > 0.05$ from one-way ANOVA with Dunnett post-test.

Dataset S4. Raw data of the siRNA deconvolution screen with CPMPs 1^{Dex} and 2^{Dex}. In this final filtering step, we prioritized siRNAs that induced significant TR changes for at least two out of the four gene-specific siRNAs (A–D) in cells treated with either CPMP **1**^{Dex} or **2**^{Dex} (or both), when compared to cells transfected with a non-targeting (RISC-Free) siRNA. siRNAs inducing significant TR changes are highlighted in blue (decrease) and red (increase). Union (final hits): 28 genes passed this filter for *either* CPMP **1**^{Dex} or **2**^{Dex}. Intersection: 9 genes passed this filter for *both* CPMPs **1**^{Dex} or **2**^{Dex}. ****$p < 0.0001$, ***$p < 0.001$, **$p < 0.01$, *$p < 0.05$, and not significant (ns) for $p > 0.05$ from one-way ANOVA with Dunnett post-test.

References

1. Lukinavicius G*, et al.* (2013) A near-infrared fluorophore for live-cell super-resolution microscopy of cellular proteins. *Nat Chem* 5(2):132-139.
2. Campeau E*, et al.* (2009) A Versatile Viral System for Expression and Depletion of Proteins in Mammalian Cells. *PLOS ONE* 4(8).
3. Maejima I*, et al.* (2013) Autophagy sequesters damaged lysosomes to control lysosomal biogenesis and kidney injury. *EMBO J* 32(17):2336-2347.
4. Holub JM, Larochelle JR, Appelbaum JS, & Schepartz A (2013) Improved assays for determining the cytosolic access of peptides, proteins, and their mimetics. *Biochemistry* 52(50):9036-9046.
5. LaRochelle JR, Cobb GB, Steinauer A, Rhoades E, & Schepartz A (2015) Fluorescence correlation spectroscopy reveals highly efficient cytosolic delivery of certain penta-arg proteins and stapled peptides. *J Am Chem Soc* 137(7):2536-2541.
6. Sinclair JK, Denton EV, & Schepartz A (2014) Inhibiting epidermal growth factor receptor at a distance. *J Am Chem Soc* 136(32):11232-11235.
7. Qian Z*, et al.* (2016) Discovery and Mechanism of Highly Efficient Cyclic Cell-Penetrating Peptides. *Biochemistry* 55(18):2601-2612.
8. Yu P, Liu B, & Kodadek T (2005) A high-throughput assay for assessing the cell permeability of combinatorial libraries. *Nat Biotechnol* 23(6):746-751.
9. Mallik B*, et al.* (2005) Design and NMR characterization of active analogues of compstatin containing non-natural amino acids. *J Med Chem* 48(1):274-286.
10. Desfougeres Y, D'Agostino M, & Mayer A (2015) A modular tethering complex for endosomal recycling. *Nat Cell Biol* 17(5):540-541.
11. Quach K, LaRochelle J, Li XH, Rhoades E, & Schepartz A (2018) Unique arginine array improves cytosolic localization of hydrocarbon-stapled peptides. *Biorg Med Chem* 26(6):1197-1202.
12. Nitsche JM, Chang HC, Weber PA, & Nicholson BJ (2004) A transient diffusion model yields unitary gap junctional permeabilities from images of cell-to-cell fluorescent dye transfer between Xenopus oocytes. *Biophys J* 86(4):2058-2077.
13. Weiss M, Hashimoto H, & Nilsson T (2003) Anomalous protein diffusion in living cells as seen by fluorescence correlation spectroscopy. *Biophysical Journal* 84(6):4043-4052.
14. Bronstein I*, et al.* (2009) Transient anomalous diffusion of telomeres in the nucleus of mammalian cells. *Phys Rev Lett* 103(1):018102.
15. Schneider CA, Rasband WS, & Eliceiri KW (2012) NIH Image to ImageJ: 25 years of image analysis. *Nat Methods* 9(7):671-675.
16. Blangy A*, et al.* (1995) Phosphorylation by p34(cdc2) regulates spindle association of human Eg5, a kinesin-related motor essential for bipolar spindle formation in vivo. *Cell* 83(7):1159-1169.
17. Malo N, Hanley JA, Cerquozzi S, Pelletier J, & Nadon R (2006) Statistical practice in high-throughput screening data analysis. *Nat Biotechnol* 24(2):167-175.
18. Zhang XD*, et al.* (2007) The use of strictly standardized mean difference for hit selection in primary RNA interference high-throughput screening experiments. *J Biomol Screen* 12(4):497-509.
19. VanNoorden CJF*, et al.* (1997) Ala-pro-cresyl violet, a synthetic fluorogenic substrate for the analysis of kinetic parameters of dipeptidyl peptidase IV (CD26) in individual living rat hepatocytes. *Anal Biochem* 252(1):71-77.
20. Dunn KW, Kamocka MM, & McDonald JH (2011) A practical guide to evaluating colocalization in biological microscopy. *Am J Physiol Cell Physiol* 300(4):C723-C742.